



Palestine Polytechnic University

Deanship of Graduate Studies and Scientific Research

Master of Civil Engineering

Strengthening of Reinforced Concrete Beam-Column Joint using CFRP
(Experimental review and Numerical modelling Study)

Student Name:
Faraj Abu Zaid

Supervisor:
Dr. Belal Almassri

Thesis submitted in partial fulfillment of requirements of the degree
Master of Civil Engineering

May, 2023

The undersigned hereby certify that they have read, examined and recommended to the Deanship of Graduate Studies and Scientific Research at Palestine Polytechnic University:

**Thesis Title: Strengthening of Reinforced Concrete Beam-Column Joint using CFRP
(Experimental review and Numerical modelling Study)**

Student Name: Faraj Abu Zaid

in partial fulfillment of the requirements for the degree of Master in Civil Engineering:

Graduate Advisory Committee:

Assistant Prof./Dr Belal Almassri (Supervisor), Palestine Polytechnic University

Signature: _____ Date: _____

Associate Prof./ Dr Riyad Awad (External committee member), Annajah National University

Signature: _____ Date: _____

Assistant Prof./Dr Haitham Ayyad (Internal committee member), Palestine Polytechnic University

Signature: _____ Date: _____

Thesis Approved by:

Name: _____

Dean of Graduate Studies & Scientific Research

Palestine Polytechnic University

Signature:.....

Date:.....

**Strengthening of Reinforced Concrete Beam-Column Joint using CFRP
(Experimental review and Numerical modelling Study)**

Student Name: Faraj Abu Zaid

ABSTRACT

Beam-column joints in RC Buildings are crucial elements in structures, especially those located in locations of medium and high seismicity. During an earthquake, a complicated combination of shear and flexural stresses acts at the same time within the joint. Shear failure of beam-column joints is identified as one of the main causes of collapse of many moments resisting RC frames, particularly those old constructed buildings. Such frames were not seismic resistant due to not sufficient reinforcement details in the beam-column joint regions. The main objective of this research is to investigate the behavior of an exterior reinforced concrete (RC) beam-column joints, a review of an experimental work will be shown and a FE modelling using commercial software ABAQUS for exterior RC joints retrofitted with CFRP sheets are also discussed, parametric study includes the CFRP and compressive strength effect will be presented at the end of the study.

تقوية مفصل العمود مع الجسر في المبنى الخرساني المسلح باستخدام الكربون فايبر بوليمر

(مراجعة تجريبية ودراسة النمذجة العددية)

اسم الطالب: فرج أبو زيد

المخلص

تعتبر مفاصل الأعمدة مع الجسور في المباني الخرسانية المسلحة من العناصر الهامة في المنشآت ، لا سيما تلك الموجودة في مواقع الزلازل المتوسطة والعالية. أثناء الزلزال ، يعمل مزيج معقد من إجهادات القص والانشاء في نفس الوقت داخل المفصل. بناء على دراسات سابقة تم تحديد فشل القص في مفاصل الأعمدة مع الجسور كأحد الأسباب الرئيسية لانهييار العديد من الاطارات الخرسانية المسلحة المقاومة للزلازل عن طريق العزوم ، خاصة تلك المباني القديمة. لم تكن هذه الإطارات مقاومة للزلازل بسبب عدم وجود تفاصيل تقوية كافية في مناطق الوصلات. الهدف الرئيسي من هذا البحث هو التحقيق في سلوك مفاصل العمود الخارجي للمباني الخرسانية المسلحة، وسيتم عرض مراجعة للعمل التجريبي ونمذجة باستخدام طريقة القطع المحددة عن طريق البرنامج التجاري ABAQUS لمفاصل خرسانية مسلحة خارجية مقواة بألواح CFRP كربون فايبر, حيث سيتم أيضا مناقشة دراسة العوامل المؤثرة في عملية التقوية و تشمل CFRP نفسها بالاضافة الى قوة ضغط الخرسانة المسلحة في نهاية الدراسة.

DECLARATION

I declare that the Master Thesis entitled” Strengthening of Reinforced Concrete Beam-Column Joint using CFRP (Experimental review and Numerical modelling Study)” is my own original work, and herby certify that unless stated, all work contained within this thesis is my own independent research and has not been submitted for the award of any other degree at any institution, except where due acknowledgement is made in the text.

Student Name: Faraj Abu Zaid

Signature: _____

Date: _____

DEDICATION

Praise be to Allah, Lord of the worlds

To the Prophet Mohammad Blessings and Peace be upon him

To my father

To my mother

To my brothers

To my sisters

To my precious wife and family

To all friends and colleagues

To my teachers

To everyone working in this field

To all of them

I literally dedicate this work

ACKNOWLEDGEMENT

First of all, praise is to Allah for helping me in making this master thesis possible despite all of obstacles especially the English language difficulties and the lack of time due to my family duties and work engagement. I would like to extend thanks to many people who helped me during my research work. Countless words are to be said in acknowledging the efforts of my enthusiastic supervisor – **Dr. Belal Almassri**. His tremendous academic support and continuous encouragement cannot be shortened in few words.

Special thanks to **Dr. Haitham Ayyad** from the Civil Engineering Department for teaching me several courses and being helpful in many ways. Many thanks to the defense committee **Dr. Riyadh Awad** the president of Tul Karem Municipality for travelling and for his efforts in reviewing my thesis.

Special gratitude is to the Civil Engineering Department and special mention goes to **Dr. Maher Amro** for encouraging me and helping me in finishing my higher education studies.

Special mention goes to my parents, brothers, sister, friends and colleagues.

List of Abbreviations

RC: Reinforced Concrete

BCJ's: Beam Column Joints

CFRP: Carbon Fibre Reinforced Polymer

FE: Finite Element

CDP: Concrete Damage Plasticity

ACI-ASCE: American Concrete Institute – American Society of Civil Engineers

FRP: Fibre Reinforced Polymer

GFRP: Glass Fibre Reinforced Polymer

NSM: Near Surface Mounted

CSA: Canadian Seismic Association

List of Figures

Figure 1 Types of Joints	5
Figure 2 Types of Forces action on RC joints	6
Figure 3 Failure modes of bent In bars.....	9
Figure 4 Failure modes of bent Up bars	9
Figure 5 Steel Jackets Strengthening details of joint (Ghobarah et al., 1996).....	10
Figure 6 Shear Angle Curves (Ghobarah et al., 1996)	10
Figure 7 Vacuum impregnation procedure (French et al., 1990)	12
Figure 8 Retrofit techniques (Bracci et al., 1995)	15
Figure 9 Comparison between tensile strength of FRP	16
Figure 10 Stress strain curve of fibre	17
Figure 11 Strengthening using CFRP (Sharif et al., 2016).....	19
Figure 12 Strengthening using CFRP (Ghobarah and Said, 2001).....	19
Figure 13 Load displacement curves for retrofitted joints (Ghobarah and Said, 2001)	20
Figure 14 Compression and tension behavior of concrete under uniaxial loading.....	23
Figure 15The yield function in 2-D plane stress (bi-axial) condition	25
Figure 16 Dilation Angle.....	27
Figure 17 Failure Surface Definition.....	28
Figure 18 Tension Compression Behavior in Concrete.....	29
Figure 19 Tension Stiffening Model	30
Figure 20 Concrete Damage Plasticity Parametrs	33
Figure 21 steel identification in the FE model.	34
Figure 22 the isotropic steel plasticity model.....	34
Figure 23 Schematic of unidirectional FRP lamina.....	35
Figure 24 Schematic view of boundary conditions and loads	38
Figure 25 Elements used in the FE model.....	39
Figure 26 Mesh Size Effect	40
Figure 27 Reinforcement Details.....	41
Figure 28 Test Set up.....	42
Figure 29 Verification of Control Specimen	43
Figure 30 The experimental crack pattern.....	44
Figure 31 FEM crack Pattern	45
Figure 32 Resin and Hardener	46
Figure 33 FEM Vs Experimental for repaired specimen RS1	47
Figure 34 Load-Displcamanet for repaired and non-repaired specimens ($f_c'=21$ MPa)	48
Figure 35Load-Displcamanet for repaired and non-repaired specimens ($f_c'=32$ MPa)	49
Figure 36 Load-Displcamanet for repaired and non-repaired specimens ($f_c'=40$ MPa)	49
Figure 37 Load Displacement FEM VS experimental for RS2 ($f_c'=21$ MPa).....	50
Figure 38 Load Displacement FEM VS experimental for RS2 ($f_c'=32$ MPa).....	51
Figure 39 Figure 38 Load Displacement FEM VS experimental for RS2 ($f_c'=40$ MPa)	51
Figure 40 load -displacement at the first stage of loading.....	52
Figure 41 Stiffness Ratio	52

List of Tables

Table 1 Plastic model parameters.....	31
Table 2The mechanical properties of concrete.....	32
Table 3 Properties of FRP sheets for joints BCJ-CFRP	37
Table 4 Properties of epoxy for installing FRP sheets for joints BCJ-CFRP	37
Table 5 Properties for combined CFRP sheets with matrix for joints BCJ-CFRP	37

Table of Contents

ABSTRACT	II
الملخص	III
DECLARATION	IV
DEDICATION	V
ACKNOWLEDGEMENT	VI
List of Abbreviations	VII
List of Figures	VIII
List of Tables	IX
Table of Contents	1
Chapter 1: Introduction	3
1.1 General Introduction	3
1.2 Research Objective.....	3
1.3 Research Methodology.....	4
1.4 Research Outline	4
Chapter 2: Literature Review	5
2.1 General Background.....	5
2.2 Design Practice of RC beam-column joint in Israel.....	7
2.3 Failure Modes in Beam-Column Joints in Old Buildings.....	8
2.4 Strengthening of RC beam-column joints.....	9
2.4.1 Steel Jacketing.....	9
2.4.2 Epoxy Repair.....	11
2.4.3 Removal and replacement	13
2.4.4 Concrete Jacketing	14
2.4.5 Strengthening of RC beam-column joints using CFRP	16
2.5 Seismic behavior of RC beam-column joints strengthened with CFRP	20
2.6 Numerical FEM studies on Beam-Column Joints using CFRP	21
Chapter 3: Finite Element FE Modelling	22
3.1 General Background.....	22
3.2 Materials Constitutive models.....	22

3.2.1 Concrete	22
3.2.2 Steel.....	33
3.2.3 Carbon Fiber-Reinforced Polymer (CFRP).....	35
3.3 Boundary Conditions.....	38
3.4 Meshing.....	39
Chapter 4: Results and Analysis.....	41
4.1 Model Verification	41
4.2 Load displacement curves for control specimens	42
4.3 Crack Patterns of specimens	43
4.4 Load displacement curves for strengthened specimens	47
4.5 Parametric study.....	48
4.5.1 Effect of CFRP with different F_c' values	48
4.5.2 Stiffness of BCJ's	52
Chapter 5: Conclusions and Recommendations	53

Chapter 1: Introduction

1.1 General Introduction

Beam column joints are one of the most critical components of reinforced concrete moment resisting frames, since it is subjected to large forces during severe ground shaking. During the last years, moderate and severe earthquake have struck different places in the world, causing severe damage to RC structure. Retrofitting of existing structures is one of the major challenges that modern civil engineering structures has demonstrated that most of them will need major repairs in the near future. Shear failure and bonding deterioration are considered as primary cause of failure of beam column joints in moment resisting framed structures. Evidences from past earthquakes have shown that failure of beam column joints often leads to partial or total collapse of structures. Hence the work of retrofitting of beam column joint using CFRP will be useful to maintain structural safety and reliability.

1.2 Research Objective

The main objective of this research is to construct a FE model in order define the behavior and strength of the BCJs a monotonic load is applied to the tip of the beam. A numerical investigation of important parameters is performed to study their influence on the behavior of an exterior BCJ. The studied parameters include (the effect of CFRP and the concrete compressive strength). The Finite element model is first verified by comparing its results with experimental results of a similar joint found in the literature.

1.3 Research Methodology

- An experimental review study will be done for both exterior and interior beam-column joints, for exterior shear deficient RC BCJs (non-strengthened and strengthened with CFRP sheets).
- Several FE numerical models will be conducted in order to validate previous experimental results for exterior beam-column joints strengthened with CFRP sheets in order to check the behaviour and failure modes/crack patterns.
- Load-displacement curves and properties such as stiffness for BCJs are discussed, for both retrofitted and non-retrofitted elements using CFRP sheets.
- Parametric Study of CFRP effect and compressive strength will be conducted.
- The commercial software ABAQUS will be used to simulate the joints according to previous experimental data, the concrete will be modelled using concrete damaged plasticity CDP model which is integrated in the program and will be discussed later.

1.4 Research Outline

The thesis consisted of five chapters, each chapter contains the followings:

Chapter 1: Introduction, Research Problem and Research Methodology

Chapter 2: Experimental Investigation in the Literature review

Chapter 3: FE Modelling Parameters, Material Properties and Boundary Conditions

Chapter 4: Results and Discussion of verification of model, load-displacement curves, crack patterns and results of parametric study

Chapter 5: Some important Conclusions and Recommendations

Chapter 2: Literature Review

2.1 General Background

Design of R.C beam-column joint is considered to be one of the crucial parts of the structure. RC beam-column joint is an important point to study in the RC structures as it is subjected to a combination of different types of loadings. The loads effects will make it difficult to predict the real behavior of the joint, especially dynamic loadings (Kaliluthin et al., 2014). The combination of such stresses due to different loadings may lead to joint's sudden failure. Therefore, RC beam-column joints must be retrofitted to prevent early and brittle failure. The ductility of the joint depends on the ultimate deformation values and the margin between this value and the yielding value which called Plasticity of the joint. By increasing the joint's ductility, the joint will be safer and in case a structural damage happened due to an accident or an earthquake, then warnings will take place and there will be sufficient time to repair the joints. There are different types of framed joints available to use in practice; such as corner-roof joint, corner joint, exterior-roof joint, exterior joint, and interior joint as shown in Figure 1.

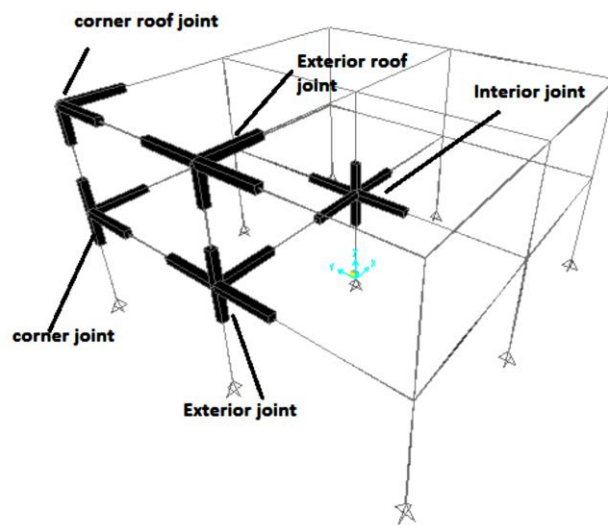


Figure 1 Types of Joints

Each joint has its unique path of behavior which is different from any other joint, due to differences in internal stresses presenting. Both normal and shear stresses act at the same time in at the joint, those stresses may lead to diagonal tension cracking or crushing in concrete in the compression side of the section as shown in Figure 2 (KR and GS, 2012). So, proposing a strengthening and reinforcing technique depends on the behavior of each type of joints.

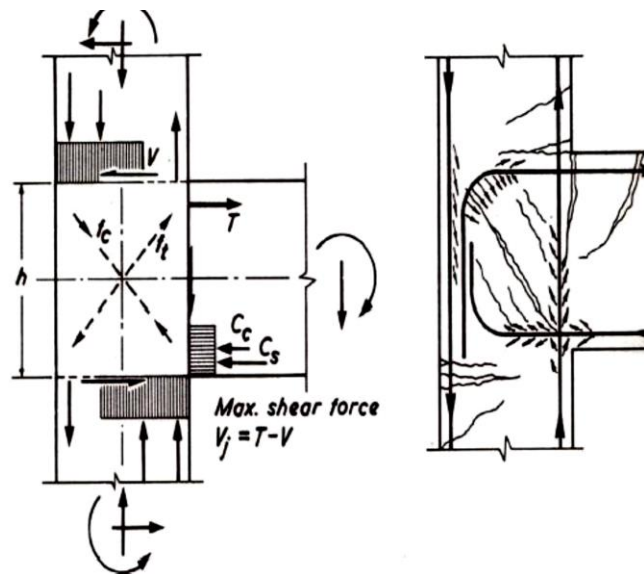


Figure 2 Types of Forces action on RC joints

Lack of ductility rather than inadequate lateral strength has been recognized as the main reason behind the deficiency in seismic performance of gravity load designed existing buildings, as a result of not defining the capacity design principles and poor reinforcement detailing (Priestley, 1997). A weak-column/strong-beam system results, with tendency to create soft-storey mechanisms, this considered to be global point of view. On the other side, insufficient protection of region within beam-column joint will result in brittle failure mechanisms of structural members.

Typical structural deficiencies can be related to:

1. Insufficient boundaries effects in the predicted plastic regions;
2. Insufficient amount of transverse reinforcement in the joint regions;
3. Insufficient amount of column longitudinal reinforcement.
4. Absence of adequate detailing, for both longitudinal and transverse reinforcement.
5. Lapped splices of column reinforcement just above the floor level;
6. Bad quality of materials (concrete and steel) such as using smooth bars which can be pulled-out easily and/or low properties of both concrete and steel.

The ACI-ASCE 352 (1985) classifies the joints in two categories based on type of design loads and deformations:

1- **Category 1:** joints are designed for ultimate strength only without considering the ductility. This type is designed for gravity and normal wind loads.

2- **Category 2:** joints are designed for sustained loadings under deformation reversals into the inelastic range. This type is designed to resist lateral loads such as earthquake, blast and cyclonic winds.

2.2 Design Practice of RC beam-column joint in Israel

Similar to other neighbor and old European countries, many of the existing residential and public buildings structures in Israel were built in periods when there was no consideration of possible seismic actions in the region. Most of these buildings were built by conventional construction methods and they considered a reinforced concrete structure with no seismic standards. Nowadays, the seismic standards and repair strategies of old RC buildings in order to improve the ultimate strength and the behavior of the structural

members is an important issue in many countries. Israel uses a nationwide statutory plan known as Tama 38 for retrofitting buildings built during the 1970s (Margalit and Mualam, 2020). According to Tama 38, building designers should add reinforced concrete (RC) stiffening elements to the retrofitted structure (Ribakov et al., 2018). Except for this classical method, there are new retrofitting methods which are expected to substitute the older ones. Installing dampers that are based on the energy dissipation principle, such as high-damping rubber bearings that isolate the structure from ground motion (Cherry and Filiatrault, 1993; Naeim and Kelly, 1999; Ribakov et al., 2018), are examples of such contemporary approaches. During the 1970s and 1980s, many residential mid-rise RC buildings in Israel were constructed with open ground floor and slender columns. These buildings usually suffer from seismic vulnerability, do not comply with the modern seismic-design codes, and therefore require suitable engineering intervention (Pushkar et al., 2022).

2.3 Failure Modes in Beam-Column Joints in Old Buildings

The following figures 3 and 4 show the modes of failure of beam column joints for both bent in and bent up bars, Shear failure of beam-column joints is identified as one of the main causes of collapse of many moment resisting RC frames, particularly those constructed before 1970's. Such frames were not seismic resistant due to the inappropriate reinforcement details within the beam-column joint regions.

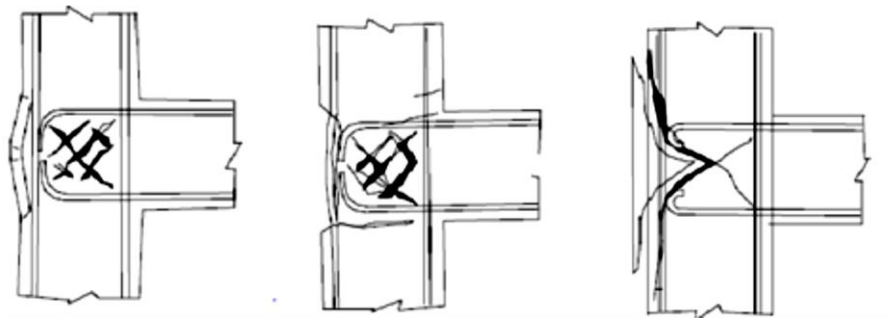


Figure 3 Failure modes of bent In bars

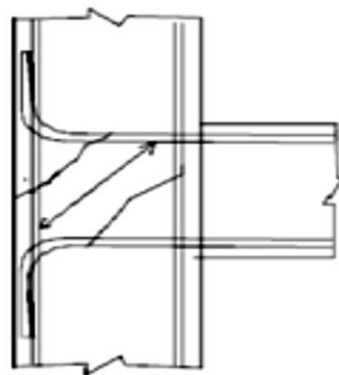


Figure 4 Failure modes of bent Up bars

2.4 Strengthening of RC beam-column joints

Due to the importance of beam column joints, there are many strengthening techniques are available to use in order to improve the behavior of each type of joints, such as steel jacketing, improving the detailing of the joint and the using the fibre polymer reinforcement FRP.

2.4.1 Steel Jacketing

Steel jacketing is a common method used to strengthen the structural members. (Ghobarah et al., 1996) experimentally tested four specimens of beam-column joints with one-third scale under cyclic loading. Specimens J1,J3 and J4 have the same detailing of reinforcement, while the reinforcement for specimen J2 was detailed according to the

Canadian seismic design code (CSA 1994). Specimens J1 and J2 were built without steel jacketing, while specimen J3 was encased by a corrugated steel jacket on the beam and column, whereas J4 encased on column only. The details of beam and column steel jackets are shown in Figure 5. The results of the experiments showed that the steel jacketing around beam and column caused remarkable increase of the ductility as shown in Figure 6.

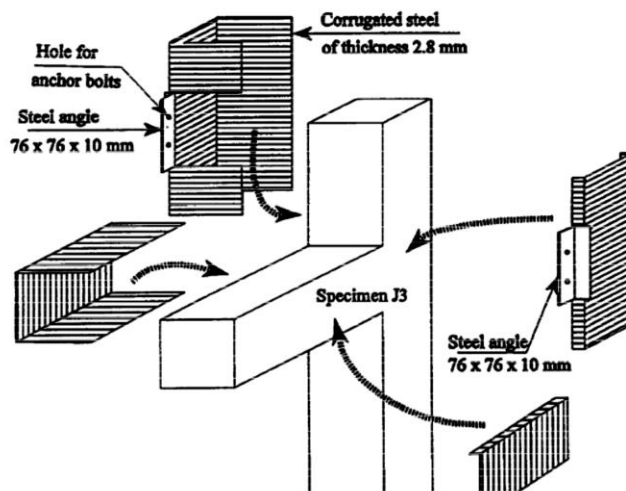


Figure 5 Steel Jackets Strengthening details of joint (Ghobarah et al., 1996)

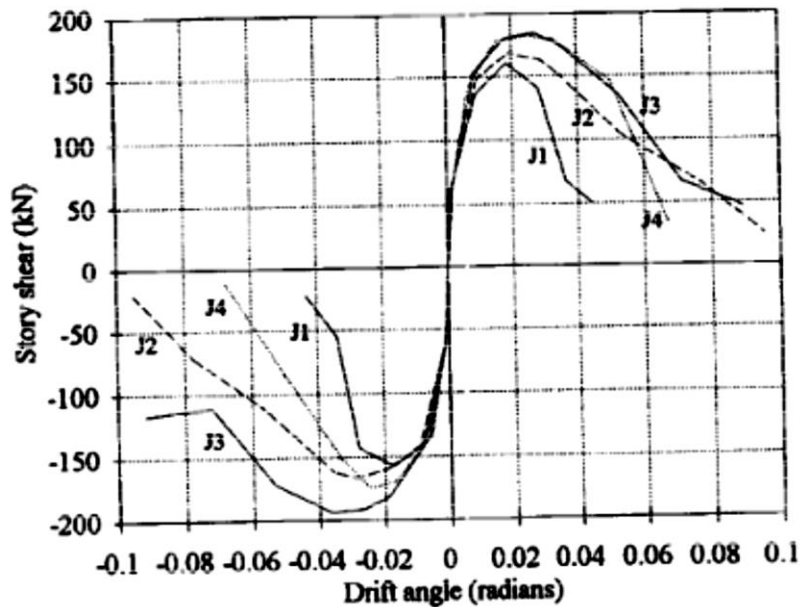


Figure 6 Shear Angle Curves (Ghobarah et al., 1996)

2.4.2 Epoxy Repair

(Jing et al., 2004) presented an experimental investigation to measure the effect of different types of joint reinforcements detailing for low to moderate seismic risk regions. All test units had the same dimensions for beam and column. Load deflection curve for each specimen was drawn. The results showed that the ductility for joint with column stirrups in joint is more than the ductility of joint without column stirrups in joint by 20%.

Reinforced Concrete structures have long been repaired using pressure injection of epoxy; a relatively new method of epoxy repair is vacuum impregnation. (French et al., 1990) studied the effectiveness of both epoxy techniques to repair two, one-way interior joints that were moderately damaged due to inadequate anchorage of continuous beam bars. For vacuum impregnation as shown in Figure 7, epoxy inlet ports were located at the bottom of each beam and at the base of the column repair region.

The vacuum was applied through three hoses attached at the top of the repair region in the column. Both repair techniques were successful in restoring over 85% of the stiffness, strength, and energy dissipation characteristics of the original specimens. Severe bond deterioration in the repaired joints occurred only one half-cycle earlier than in the original specimens. The main conclusion was that vacuum impregnation presents an effective means of repairing large regions of damage at once and that it can be modified for joints with fewer accessible sides.

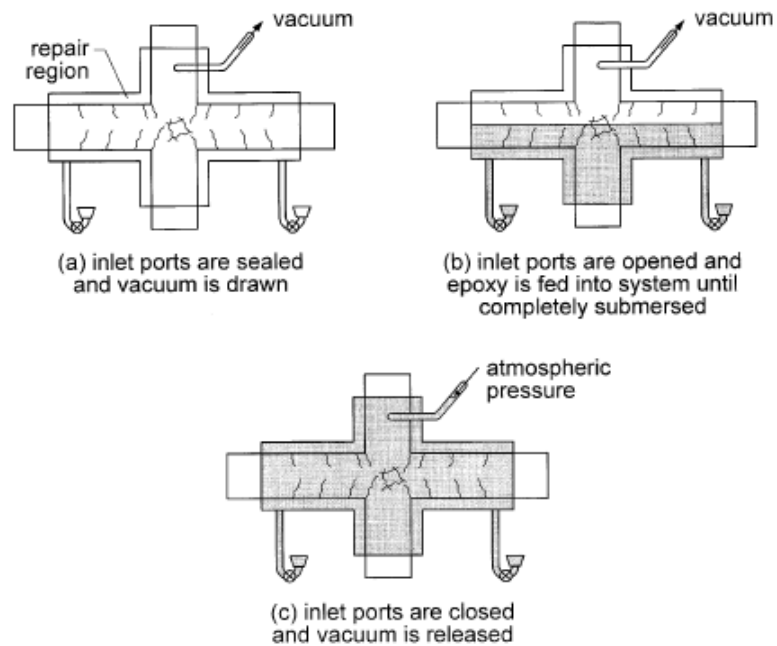


Figure 7 Vacuum impregnation procedure (French et al., 1990)

(Beres et al., 1992) retested one of their deficiently detailed oneway interior joints after repairing it by vacuum injection of methyl-methacrylate resin without removing the initially applied gravity load. The failure in both the original and repaired specimens was due to pullout of the embedded beam bottom bars and extensive diagonal cracks in the joint. Although the repair restored only 75% of the initial stiffness and 72% of the column shear capacity, the energy dissipation capacity remained almost unchanged due to a reduced rate of strength deterioration. (Filiatrault and Lebrun, 1996) reported on the performance of two one-way exterior joints, one with non-seismic detailing and one with closely spaced transverse reinforcement in the beam, column, and joint; each was repaired by epoxy pressure injection. (Filiatrault and Lebrun, 1996) said that the repair procedure was particularly effective in improving the strength, stiffness, and the energy

dissipation capacity of the no seismically detailed specimen and that more pinching was observed in the hysteresis loops of the seismically detailed specimen after repair. (Karayannis et al., 1998) studied the effects of joint reinforcement arrangement on the efficiency of epoxy repair by pressure injection. Eleven of the tested one-way exterior joint specimens were repaired by epoxy injection only and then retested. In these specimens, cracks were observed both at the joint region and at the beam end during the first cycles, but the failure was finally due to beam hinging. After repair, the specimens with two joint stirrups or column longitudinal bars crossed within the joint exhibited only beam flexural failure with serious fragmentation of concrete at the beam end and significant reduction in pinching of the hysteresis loops. The specimens with one joint stirrup, however, exhibited the same failure mode before and after repair. The increases in peak load and dissipated energy were 8 to 40% and 53 to 139%, respectively. The change in stiffness varied between a 27% decrease and a 10% increase. The variations in performance were partially attributed to the variations in being able to inject epoxy successfully into the joint cracks.

2.4.3 Removal and replacement

Partial or total removal and replacement of concrete is used for heavily damaged joints with crushed concrete, buckled longitudinal bars, or ruptured ties. Before the removal, the damaged structure must be temporarily supported to ensure stability. Depending on the amount of concrete removed, some additional ties or longitudinal reinforcement may be added. (United Nations Industrial Development Organization, 1983). Generally, high-strength, low- or nonshrink concrete is used for replacement. Special attention must be paid to achieving a good bond between the new and the existing concrete.

(Karayannis et al., 1998) tested six one-way exterior joint specimens that showed a concentrated damage in the joint and a loss of considerable amount of concrete in this region. This damage mode can be attributed to the joint not having any stirrups in two of the specimens and to the flexural strength ratio being very low (0.67) in the others. The joints were repaired by first recasting the missing part of the joint with a high-strength (83 MPa [12,100 psi]), low-shrink cement paste, then by epoxy injection into the surrounding cracks. The repair did not alter the failure mode of the specimens with one or no joint stirrups, although an increase of 39 to 71% in peak load, 15 to 39% in stiffness, and 19 to 34% in energy dissipation capacity was observed. The specimens with two joint stirrups, however, improved remarkably after repair and developed a beam hinge with no damage to the joint. On average, the peak load and the dissipated energy increased by 42 and 170%, respectively, while only 80% of the stiffness could be recovered.

2.4.4 Concrete Jacketing

One of the earliest and the most common solutions for rehabilitation of concrete frames is to encase the existing column, along with the joint region, in new concrete with additional longitudinal and transverse reinforcement. The continuity of the added longitudinal bars through the joint requires opening the slab at the column corners. The addition of the joint transverse reinforcement makes the process even more labor-intensive, in which case the beams are also cored, and in-place bending of the hooks is necessary. (Corazao and Durrani, 1989) strengthened three single (two exterior: ER, ES1R; one interior: IR) and two multi-joint (two-bay) sub assemblages (CS2R, CS4R), some including a floor slab, by jacketing the column, the joint region, and sometimes a portion of the beam. Due to the difficulties experienced with in-place bending of the crosstie hooks in the joint region, the additional joint reinforcement was modified to a set

of dowels with a hook. The strength, stiffness, and energy dissipation capacity of all three single-joint specimens were increased, except for the one-way exterior joint that enlarged joint. For both specimens, cracking near the joint dissipated less energy after jacketing. In two of these specimens, the damage was successfully moved away from the joint due to added beam bottom bars hooked both in the joint and at 25 cm (10 in.) from the column face. The retrofit was not as effective in improving the behavior of the multipoint specimens; the results were taken to indicate that jacketing of the columns alone was not adequate in restoring the performance without addressing the problem of load transfer between beams and columns.

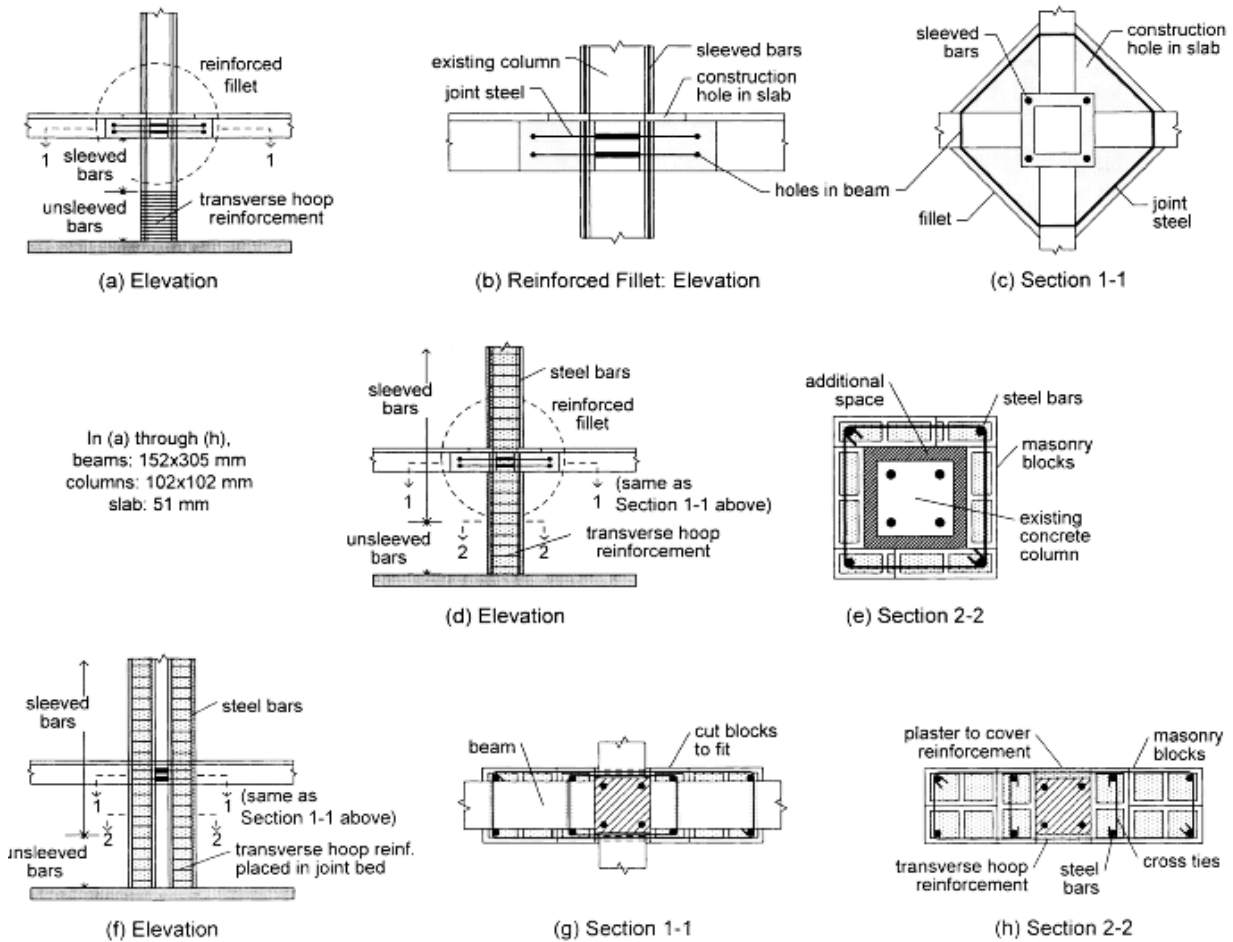


Figure 8 Retrofit techniques (Bracci et al., 1995)

2.4.5 Strengthening of RC beam-column joints using CFRP

In the last years, the use of Fiber Reinforced Polymer (FRP) composites showed an effective technique for strengthening and repair reinforced concrete structures besides the use of steel jacketing. FRP is a composite material made of a polymer matrix and is reinforced with fibers. The FRP sheets are typically bonded to the structures using proper epoxy (adhesive) material. The use of FRP is a matter of adding low-weight, high-tensile strength material to the structure. This material is used especially for strengthening and retrofiting parts of structures where principal tensile stresses exceed tensile strength of the element at that location. Generally, four types of FRP are used to strengthen structures: Sprayed and Electrical Glass FRP (S-GFRP and E-GFRP), Basalt FRP (BFRP), Aramed FRP (AFRP) and Carbon FRP (CFRP). Comparison between tensile strength of those types is presented in Figure 9.

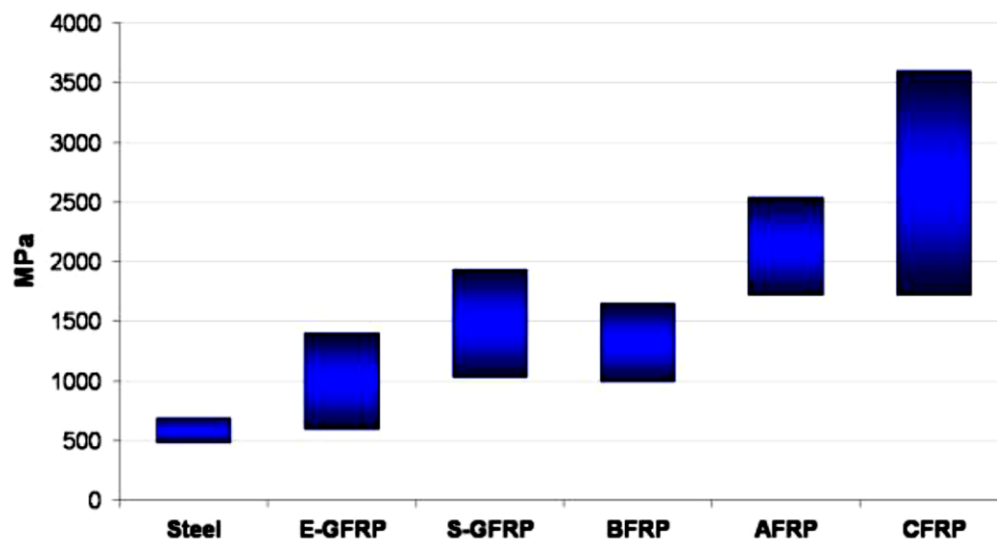


Figure 9 Comparison between tensile strength of FRP

Generally, the fibers can have a high-tensile strength of 3500 MPa, while a typical polymeric matrix normally has a tensile strength of only 35 to 70 MPa. This matrix make the overall tensile capacity of FRP less than that of pure fibers as shown in Figure 10 (Campbell, 2010).

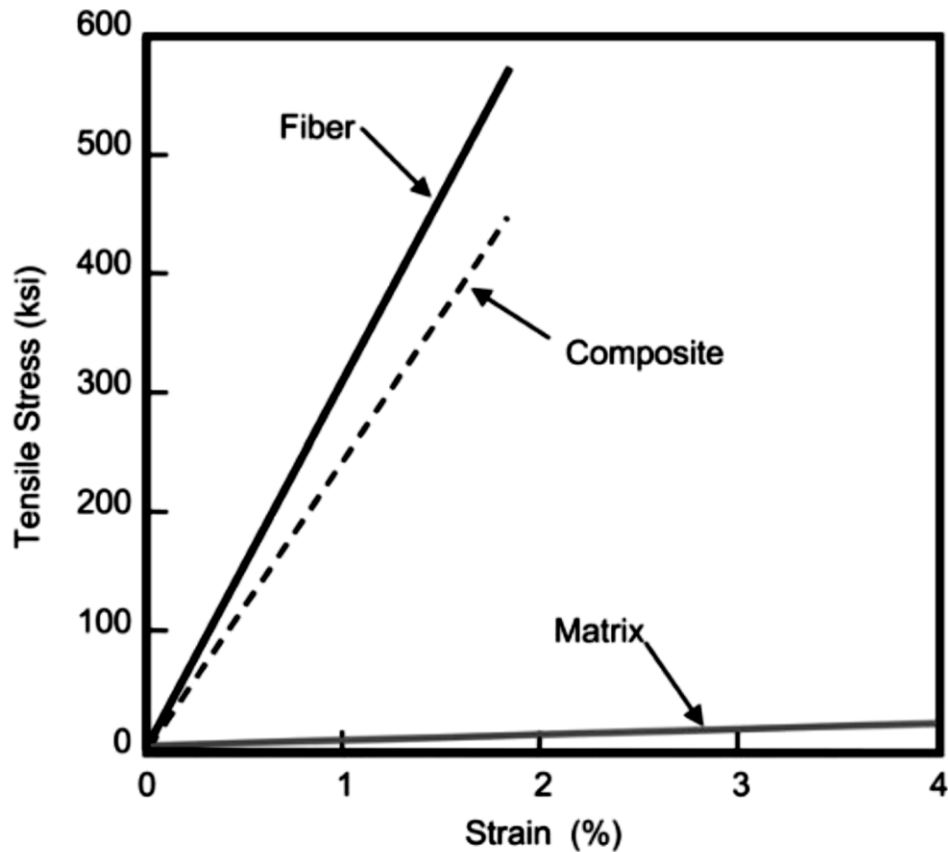
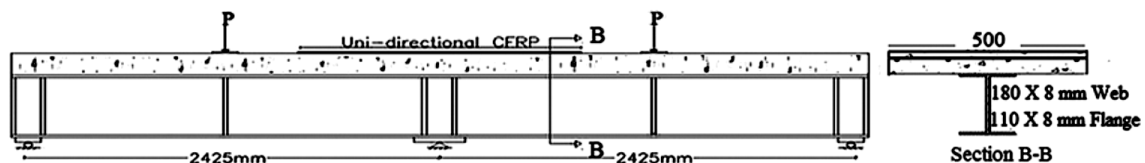


Figure 10 Stress strain curve of fibre

Different methods of retrofitting RC joints using FRP are available; sheets, laminates, strips or rebar. Extensive research was conducted on using FRP in strengthening and

retrofitting of different structural elements. (Sharif et al., 2016) presented an experimental investigation to study the effect of CFRP on the ratio between cracking load and yielding load of the continuous composite steel girders. The study aimed to maintain the composite action of the negative moment region. Three retrofitting schemes were used: First, CFRP sheets were used to maintain the composite action at the region of negative moment as shown in Figure 11. The second scheme, CFRP sheets wrapped at positive moment region as shown in Figure 11. Third scheme, CFRP sheets were used at positive and negative moment in the continuous composite steel girders. RG girder was control specimen without CFRP, while girders G1,G2 and G3 presented the first scheme of retrofitting with 1, 2 and 3 layers of CFRP, respectively. On the other hand, girder PGR showed second scheme of retrofitting. Moreover, girder G2R presented the third scheme of retrofitting with two layers of CFRP at negative moment and wrapping concrete of the moment region. Results of this investigation showed that using 1, 2 and 3 layers of CFRP at negative moment region, increases the cracking load to be 0.47, 0.75, and 0.79 of the service load for G1,G2 and G3, respectively compared to 0.86 for G2R. Also, results showed that when using CFRP only at positive moment regions, the ratio decrease from 0.47 to 0.38 due to increasing the yielding load and decreasing cracking load. However, when using CFRP at negative and positive moment regions, the ratio increased from 0.38 to 0.82. This could be summarized by showing ability of CFRP to maintain composite action at negative moment region and ability of wrapping and confining concrete slab at the moment region.



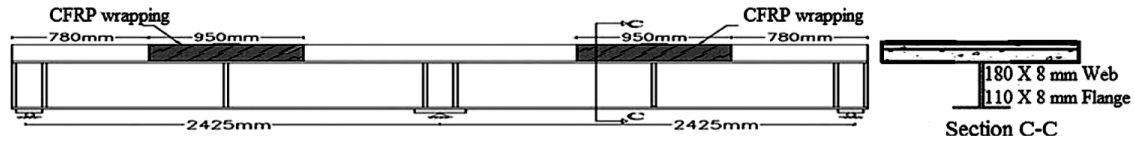


Figure 11 Strengthening using CFRP (Sharif et al., 2016)

(Ghobarah and Said, 2001) experimentally tested two full-scale specimens of exterior R.C beam column joint with to study the effect of GFRP on the behavior of joint. Specimen T1 was a control joint with no shear reinforcement within the joint region as shown in Figure 2.15. After testing joints T1, The joint was repaired and rehabilitated using GFRP as shown in Figure 2.16, and then another test was conducted. The repaired and rehabilitated specimen is designated T1R. Both specimens were placed in the testing machine, then a constant axial load with value $0.2 A_g f_c$ was applied to the column and kept constant throughout the test, and after that, a reversal cycling displacements were applied to the free end of the beam as shown in Figure 12, Results show that using GFRP within the joint leads to increasing the ductility by 60% as shown in Figure 13.

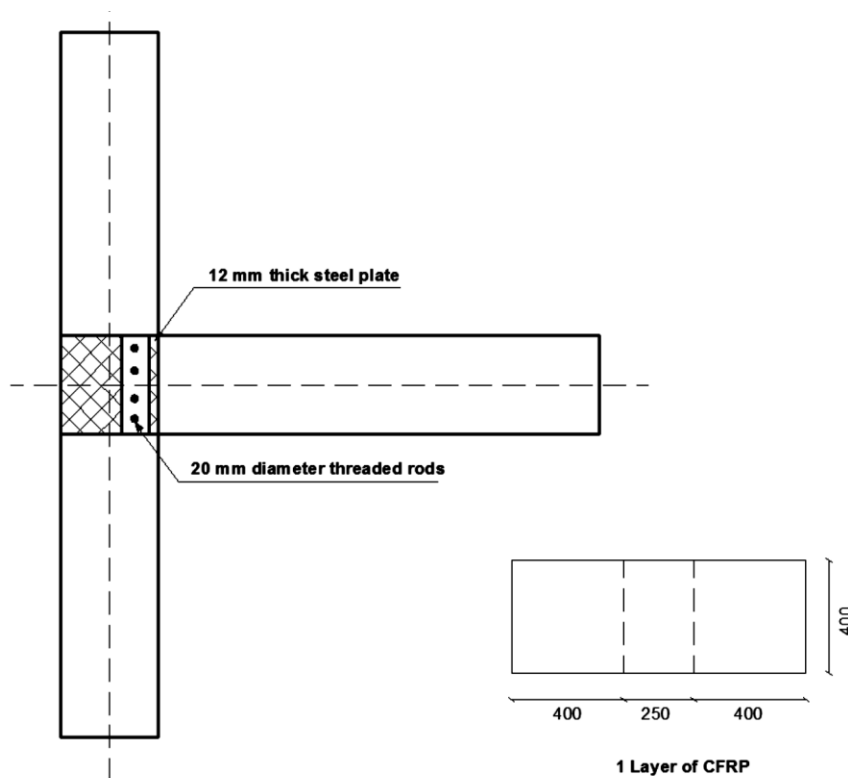


Figure 12 Strengthening using CFRP (Ghobarah and Said, 2001)

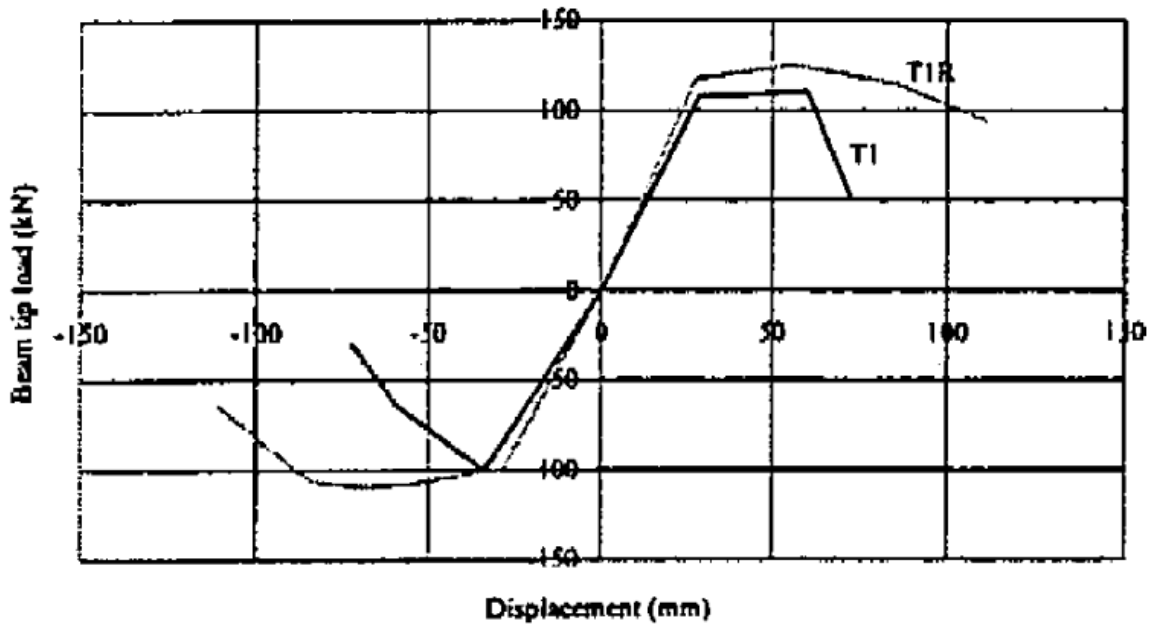


Figure 13 Load displacement curves for retrofitted joints (Ghobarah and Said, 2001)

2.5 Seismic behavior of RC beam-column joints strengthened with CFRP

Experimental results from the literature have indicated that CFRP sheets as a composite material can enhance the seismic performance of deficient beam-column joints in terms of peak horizontal load, energy dissipation, stiffness and joint shear strength. Shear distortions within the joints are significantly reduced for the strengthened specimens.

In the past, numerous research works were reported on the applications of advanced concrete materials for enhancing the strength of RC structural elements. Prota et al. (2000), have studied seismic upgrade of beam column joint using FRP reinforcement. They proposed a new technique for seismic upgrading of RC beam column connections.

This technique is based on the combined use of FRP laminates and near surface mounted bars. The FRP rods provide flexural strengthening, whereas the lay-up laminates provide confinement and shear strengthening.

Tsonos (2008) has provided the structural engineers with useful information about the safety of new RC frame structures that incorporate seismic details from current building codes. Tsonos (2008) has studied experimentally and analytically the effectiveness of RC jacket and a high strength fiber jacket for cases of the post-earthquake and pre-earthquake retrofitting of beam-column joints. He also compared the effectiveness of the two jackets. Ghobarah and El-Amoury (2005) developed effective rehabilitation systems using composite materials and steel elements to upgrade the seismic resistance to bond-slip of bottom steel bars anchored in the joint zone and to upgrade the shear resistance of joints.

2.6 Numerical FEM studies on Beam-Column Joints using CFRP

Finite element (F.E) produces an attractive solution of investigating structures effectively. Numerical investigation of effect of CFRP bars using NSM technique to maintain the mechanical capacity of corroded RC beams using different hybrid repair techniques were presented before for by Almassri et al. (2020), the study showed the possibility of adding external steel plate to an existing NSM CFRP technique in order to prevent the brittle and early mode of failure occurred by the separation of concrete cover, the concrete was modelled using concrete damaged plasticity model CDP which was integrated in Abaqus . Results showed that the beam capacity and stiffness increase with the use of NSM CFRP bonded to the top of the concrete slab at the negative moment region; the increase in ultimate capacity is directly proportional to CFRP thickness up to certain thickness, when the negative moment capacity is close to the positive moment capacity. Numerical

analysis of exterior beam-column joint was conducted by Bidgar and Bhattacharya (2014), and showed that the axial load on column makes a slight increase in the beam resisting moment capacity.

Chapter 3: Finite Element FE Modelling

3.1 General Background

Finite Element based numerical investigation of reinforced concrete buildings offers an attractive technique of research due to low cost, quick results and ability to study several variables in depth. Therefore, a three-dimensional non-linear F.E joint model is built using commercial software ABAQUS.

This chapter describes a general introduction of R.C beam-column joint modeling, as well as the material parameters for this model will be shown also in this chapter. The modeling of the joint includes definition of materials, creation of parts, modeling of interfaces, selection of analysis regime, loading setup, boundary conditions and meshes as it will be discussed in the following subsections.

3.2 Materials Constitutive models

In this section, constitutive models used in the FE modelling for concrete and steel under compression and tension loads are shown. Also, a constitutive model for fiber reinforced polymer FRP materials is included.

3.2.1 Concrete

Concrete is non-homogenous material and it is difficult to be modeled due to the non-linearity of this material and the damage behavior in tension and compression. The concrete crushing can be modelled using different ways. One of these ways is Mohr column circle and Drucker prager method, one of the ways which include crushing and

damages effects in the stress-strain behavior of concrete in what is called the —Concrete Damaged Plasticity model (CDP).

The CDP model available in ABAQUS software is used to model the complicated nonlinear behavior of concrete. In this model, two main failure criteria are considered: tensile cracking and compressive crushing of the concrete material. Compression and tension behavior of concrete under uniaxial loading is shown in Figure 14.

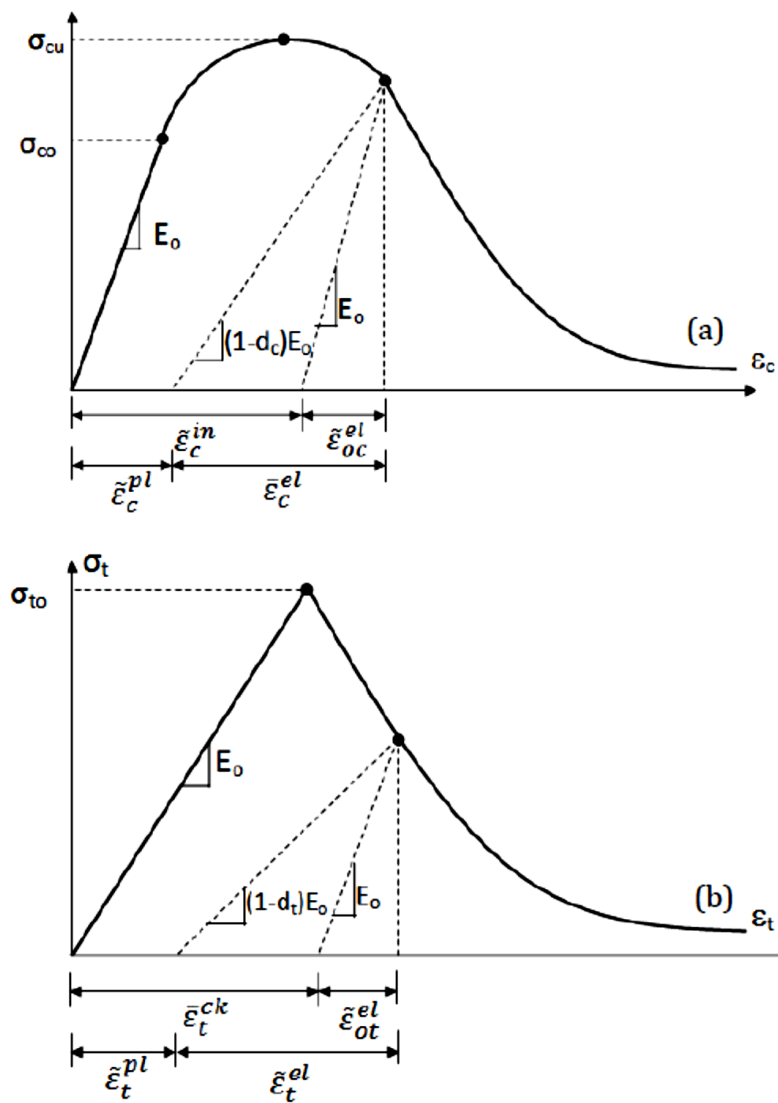


Figure 14 Compression and tension behavior of concrete under uniaxial loading

The CDP allows capturing of strength and stiffness degradation through tension and compression damages parameters (dt, dc) of concrete as shown in Figure 14 (ABAQUS User Manual, 2013).

As shown in Figure 14 the unloaded response of concrete specimen is weakened because the elastic stiffness of the material is damaged or degraded due to cracks. The degradation of the elastic stiffness on the strain softening branch of the stress-strain curve is characterized by two damage variables, dt and dc, which can take values from zero to one. Zero represents the undamaged material where one represents total loss of. E0 is the initial (undamaged) elastic stiffness of the material and $\epsilon_{c\sim pl}$, $\epsilon_{t\sim pl}$, $\epsilon_{c\sim in}$, $\epsilon_{t\sim in}$ are compressive plastic strain, tensile plastic strain, compressive inelastic strain and tensile inelastic strain respectively. The elastic relations under uniaxial tension (σ_t) and compression (σ_c) are taken into account in Equation (3.1) and Equation (3.3)

$$\sigma_t = (1-dt).E0.(\epsilon_t - \epsilon_{t\sim pl}) \quad (3.1)$$

$$\sigma_c = (1-dc).E0.(\epsilon_c - \epsilon_{c\sim pl}) \quad (3.2)$$

Where the effective tensile and compressive cohesion stress which are used to determine the yield point according to the yield function. The model makes use of the yield function according to Lubliner et al. (1989). with the modifications proposed by Lee and Fenves (1998). to account for different evolution of strength under tension and compression under multi-axial loading case. The yield function in 2-D plane stress (bi-axial) condition for instance is shown in Figure 15.

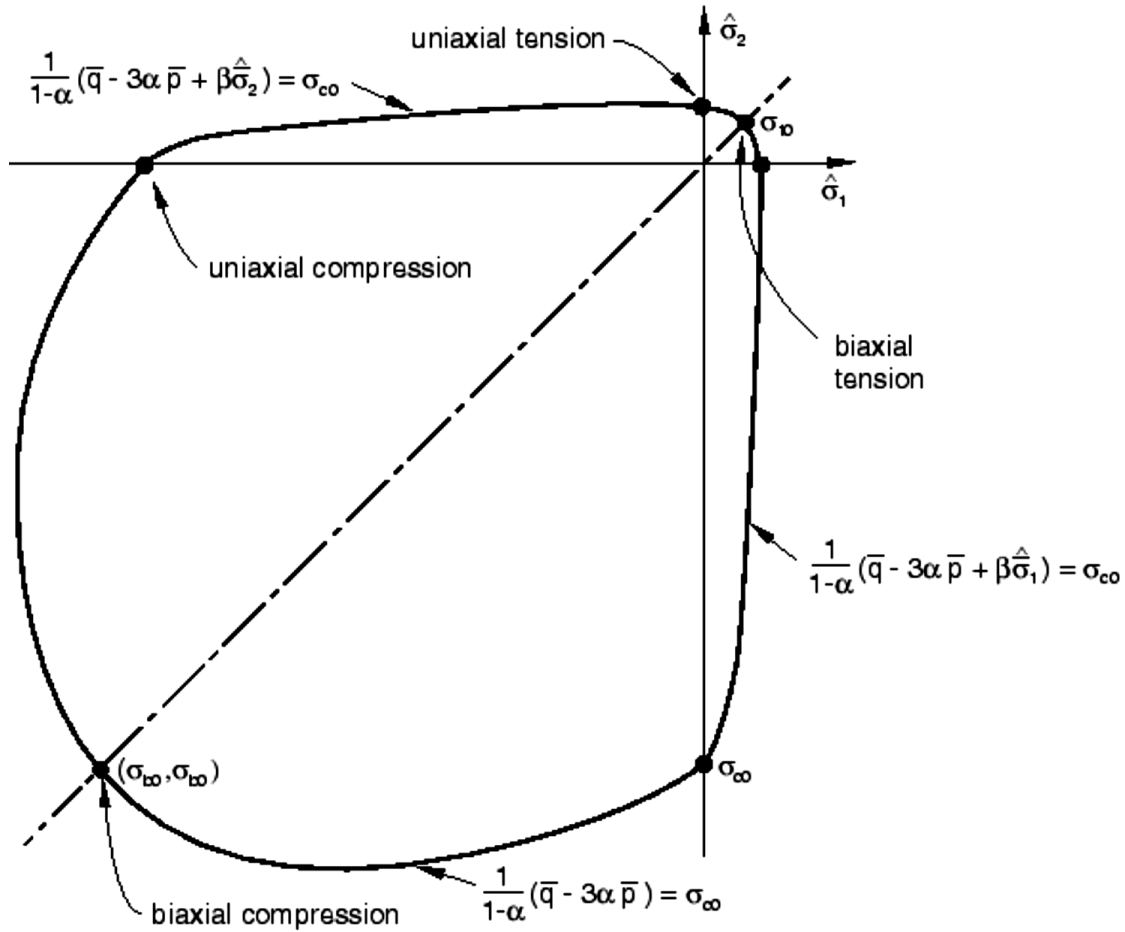


Figure 15 The yield function in 2-D plane stress (bi-axial) condition

Therefore, the material model captures the confinement effect that results from tri-axial stress data in concrete allowing improvement of compressive capacity in the case of hydrostatic stress state.

Uniaxial compression behavior

Generally, a lot of researches suggested equations that describe the behavior of concrete under uniaxial compression stress. However, most of equations do not describe full stress-strain curve of concrete, so that, the stress-strain equation proposed by Saenz

(1964) is used to define full behavior of concrete under uniaxial compressive stress.

Equation (3.3) shows the uniaxial stress-strain curve under compressive stress.

$$\sigma_c = \frac{E_c \varepsilon_c}{1 + (R + R_E - 2) \frac{E_c}{E_0} - (2R - 1) \left(\frac{E_c}{E_0}\right)^2 + R \left(\frac{E_c}{E_0}\right)^3} \quad (3.3)$$

$$E_c = 4700 \sqrt{f'_c} \quad (3.4)$$

$$R = \frac{R_E (R_\sigma - 1)}{(R_E - 1)^2} - \frac{1}{R_E} \quad (3.5)$$

$$R_E = \frac{E_c}{E_0} \quad (3.6)$$

$$R_\sigma = \frac{f'_c}{\sigma_f} \quad (3.7)$$

$$R_\varepsilon = \frac{\varepsilon_f}{\varepsilon_0} \quad (3.8)$$

$$E_0 = \frac{f'_c}{\varepsilon_0} \quad (3.9)$$

Tension behavior

The stress-strain curve for concrete under tension is tested experimentally by Sharif et al. (2015) for concrete 25MPa. The maximum tensile stress was reported as 2.9MPa corresponding to modulus of rupture of concrete which is equal $0.62\sqrt{f'_c}$ according to ACI 318, after this load, the flexural capacity of concrete started to decrease until ultimate strain reach 0.003 . Asran et al. (2016) used this equation for definition of tension behavior of concrete in ABAQUS, also assuming linear descending of tension. In this model, an assumption of maximum tensile strain of 0.003 under flexural test for all types of concrete is considered. This assumption is used due to lack of sufficient information about ultimate strain in tension of concrete from experimental tests which will be used for verification purpose.

Modeling of concrete needs many parameters according to CDP in order to capture the behavior of concrete accurately. These parameters are summarized below:

- 1- Young's Modulus (E_c): Modulus of elasticity of concrete (MPa). Equation (3.4)
- 2- Poisson's Ratio (ν) : the amount of transversal elongation divided by the amount of axial elongation. A value of 0.2 is used in the model.
- 3- Dilation angle (internal friction angle). In other words, it is the angle measured in the p - q plane (hydrostatic pressure stress - Mises equivalent effective stress) at high confining pressure as shown in Figure 16 (ABAQUS User Manual, 2013). In simulations usually $\psi = 36^\circ$ or 40° is recommended by Kmiecik and Kaminski (2011).

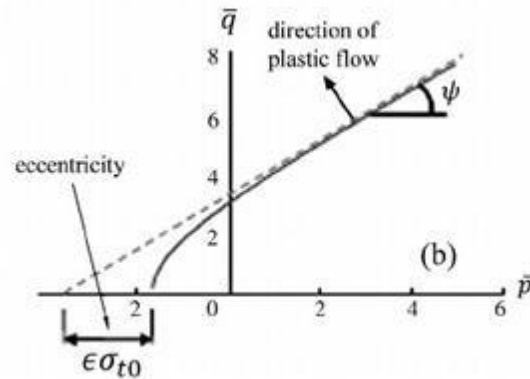


Figure 16 Dilation Angle

- 4- Eccentricity: parameter that defines the rate at which the flow potential function approaches the asymptote in p - q plane. The CDP model recommends assuming this value equal 0.1 (ABAQUS 2008). When this value equals 0 then the surface in the meridian plan becomes straight line similar to the classic Drucker-Prager hypothesis as shown in Fig(3.10) (ABAQUS 2008).
- 5- f_{b0}/f_{c0} : bi-axial compression stress divided by uni-axial compression stress. Kupfer (1969) conducted experimental test and obtained that this ratio is best used equal to 1.16.

6- K : represents the ratio of the distances between the hydrostatic axis and both the compression and the tension meridians in the deviatoric cross section which is equal $2/3$ which is recommended by ABAQUS (2008). This factor is used to convert the shape of cross section of failure surface from circle to combination of three mutually tangent ellipse as shown in Figure 17 (ABAQUS User Manual, 2013). This shape was formulated by William and Warkne (1975).

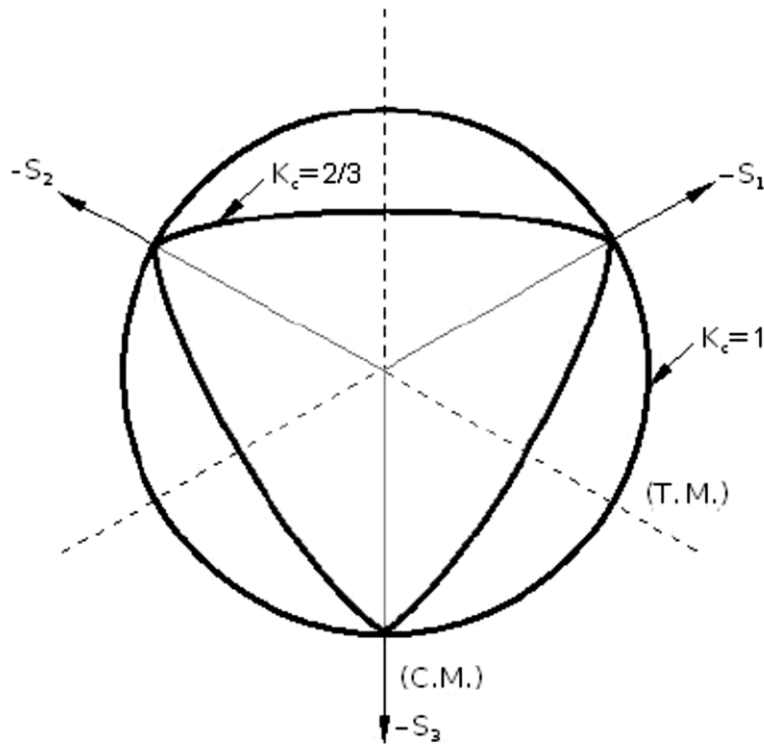


Figure 17 Failure Surface Definition

7- Compression stress versus inelastic strain curve: Compression yield stress versus inelastic strain curve used in this thesis as an input data for definition CDP model.

8- Tension yield stress versus cracking strain curve: Tension yield stress versus Cracking strain curve used in this thesis is thesis as an input data for definition CDP model.

9- Compression damage parameter: This parameter represents the degradation of the elastic stiffness due to compression in concrete. is defined as the ratio between the inelastic strain (crushing strain) and total strain (Wahalathantri et al. 2011).

10- Tension damage parameter (d_t): This parameter represents the degradation of the elastic stiffness due to tension in concrete. d_t is defined as the ratio between the cracking strain and total strain (Wahalathantri et al. 2011).

11- Tension recovery (ω_t) and compression recovery (ω_c): These are material properties that control the recovery of the tensile and compressive stiffness upon load reversal. The experimental observation in most quasi-brittle materials, including concrete, is that the compressive stiffness is recovered upon crack closure as the load changes from tension to compression. On the other hand, the tensile stiffness is not recovered as the load changes from compression to tension once crushing micro-cracks have developed. This behavior, which corresponds to $\omega_t = 0$ and $\omega_c = 1$, is the default used by ABAQUS. Uniaxial load cycle (tension-compression-tension) with default values for the stiffness recovery factors: to $\omega_t = 0$ and $\omega_c = 1$ as shown in Figure 18 (ABAQUS User Manual, 2013).

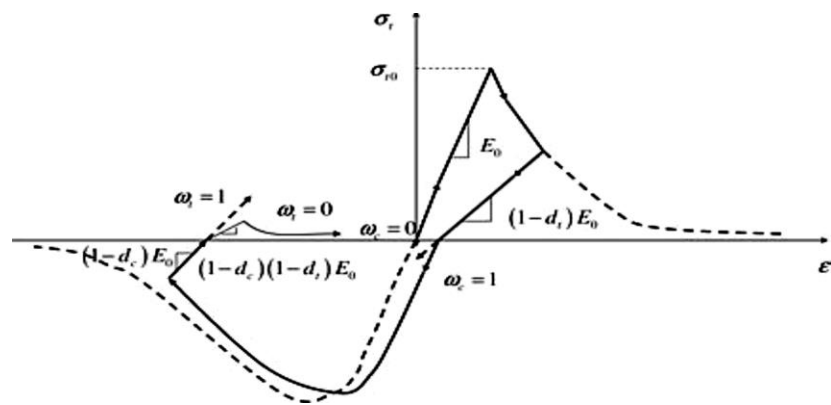


Figure 18 Tension Compression Behavior in Concrete

In order to predict the behavior of concrete under tensile stress, Nayal and Rasheed 2006 proposed a model that reflects the response of concrete for the full range of strains. Based on this model, a sharp change in deformation may occur at some point due to a sharp drop in stress. For this reason, the curve was corrected by Wahalathantri et al. 2011, and it led to better results. Fig. 19 a and b show the original and the corrected versions of the model.

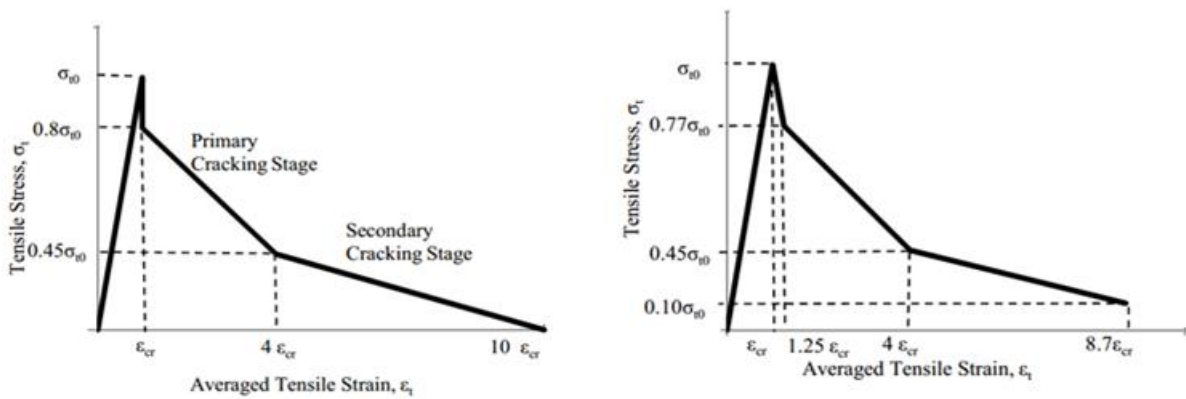


Figure 19 Tension Stiffening Model

a) (Nayal and Rasheed 2006) model
et al.2011)

b) Modified model by (Wahalathantri

ACI 318 code suggests that the maximum uniaxial tensile stress (σ_{t0}) is equal to $0.31\sqrt{f'_c}$, which corresponds to the cracking strain (ϵ_{cr}).

The CDP model requires the values of four main parameters to be identified. The parameters are the dilation angle ψ measured in the p-q plane at a high confining pressure; σ_{t0} is the uniaxial tensile stress at failure; and ϵ which denotes the eccentricity

that defines the rate at which the function approaches the asymptote (as the eccentricity approaches zero, the flow potential converges to a straight). In the work of Voyiadjis and Taqieddin 2009 it was mentioned that the range of the dilation angle (ψ) in the CDP model can be taken between 31 and 42. For the purpose of performing simulations, Kmiecik and Kaminski 2011 recommend a value of 36° (which is selected for this research) or 40° for the dilation angle (ψ). Finally, the viscoplastic regularization is defined by the viscosity (μ) which takes the value of zero. However, to prevent the occurrence of convergence problems, this parameter is given a very low value (0.0001).

Table 1 summarizes the values selected in this research for the plastic model parameters of concrete. The two uniaxial damage variables d_t and d_c define the degradation of concrete. These independent quantities are assumed varying according to the plastic strains. In this study, these parameters are calculated by using the equations developed by Jankowiak & Lodygowski (2005).

The mechanical properties of concrete are shown in Table 2. The curves shown in Fig. 20 a and b represent the stress-strain relations for concrete. The damage-strain relations are shown in Fig. 20 c and d. The FEM analysis is based on these curves.

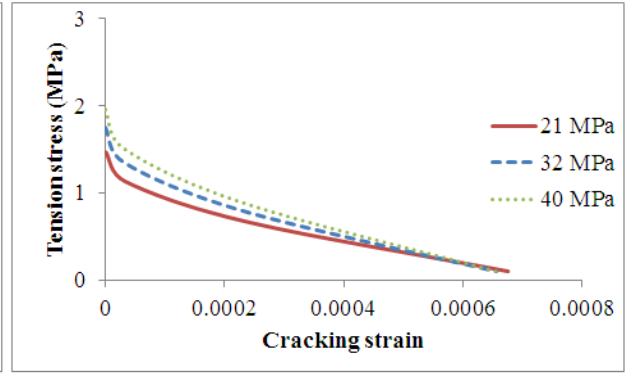
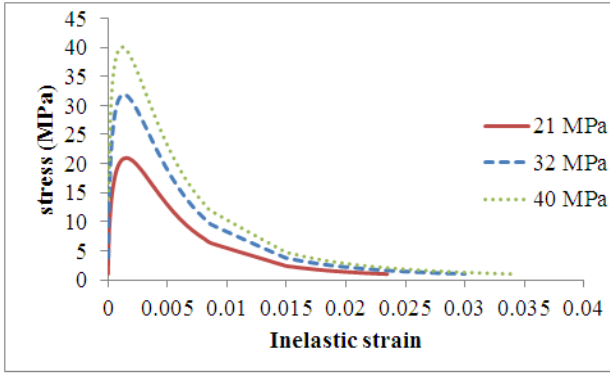
Table 1 Plastic model parameters

Parameter name	Value
Dilation angle (ψ)	36°
Eccentricity (e)	0.1

f_{b0}/f_{c0} (ratio of initial equibiaxial compressive yield stress to initial uniaxial compressive yield stress)	1.16
K (the ratio of the second stress invariant on the tensile meridian)	0.667
Viscosity Parameter	0

Table 2 The mechanical properties of concrete

Concrete Type	Compressive strength (MPa)	E (MPa)	v
Concrete I	21	21500	0.2
Concrete II (parametric + verification)	32	26600	0.2
Concrete III	40	29700	0.2



(a) Compressive stress vs. Inelastic strain

(b) Tensile stress vs. Cracking strain

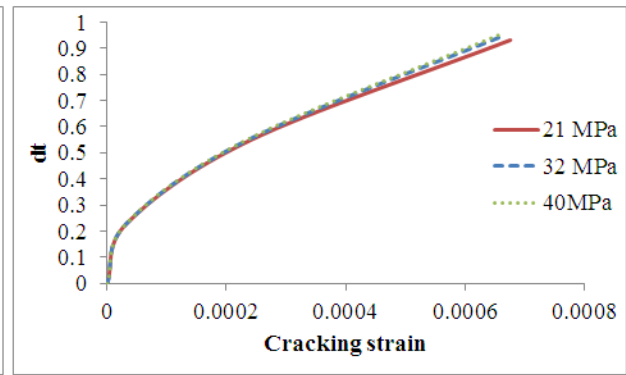
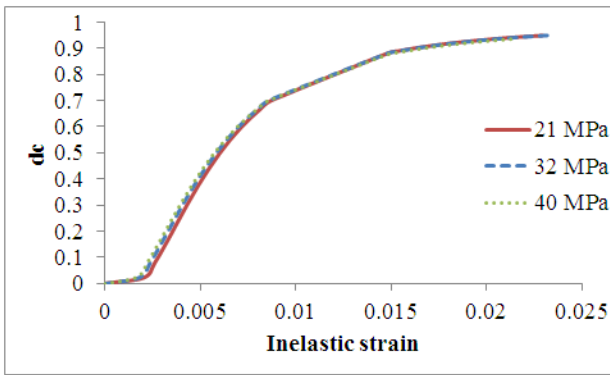


Figure 20 Concrete Damage Plasticity Parameters

(c) Compressive damage vs. Inelastic strain (d) Tensile damage vs. Cracking strain

3.2.2 Steel

Generally, steel is initially linear-elastic for stress less than the initial yield stress. At ultimate tensile strain, the reinforcement begins to neck and strength is reduced. At a maximum strain, the steel reinforcement fractures and load capacity is lost, Figure 21 presents the ideal stress-strain curve of the steel identification in the FE model.

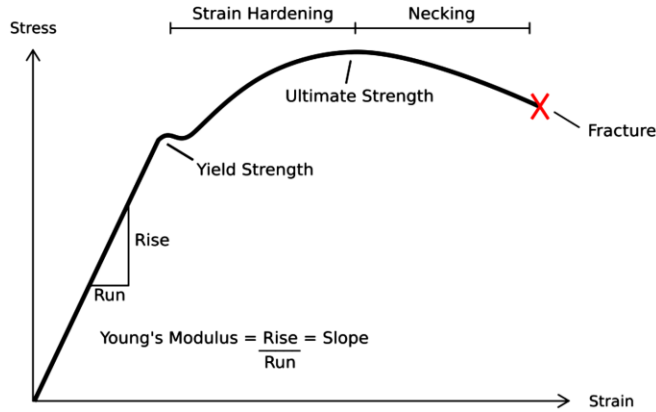


Figure 21 steel identification in the FE model.

An isotropic behavior was used to model the reinforcement and loading plate. This means that the yield surface changes size uniformly in all directions such that the yield stress increases (or decreases) in all stress directions as plastic straining occurs. For Steel reinforcement, an elastic modulus of elasticity of 200000 MPa is used to define the elastic behavior of steel until yield strain. In order to model steel material after yield strain, the isotropic plasticity model is used, as shown in Figure. 22.

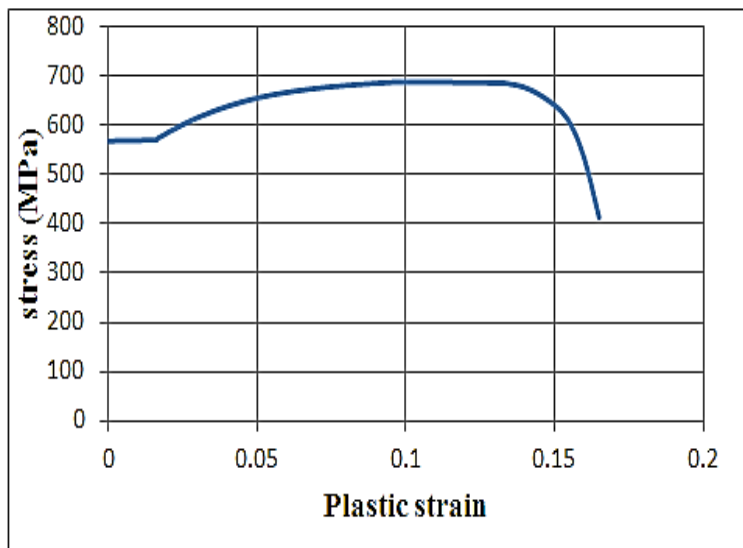


Figure 22 the isotropic steel plasticity model

3.2.3 Carbon Fiber-Reinforced Polymer (CFRP)

Unidirectional FRP sheets were assumed to strengthen the R.C beam-column joint model.

The fibers provide both load carrying capacity and stiffness to the FRP composite sheet while the matrix is to ensure distribution of the load among all fibers and to protect the fibers themselves from the environment. The fiber behavior is assumed linear elastic up to failure with rupture failure. A lamina linear elastic element is used to model CFRP as shown in Figure 23.

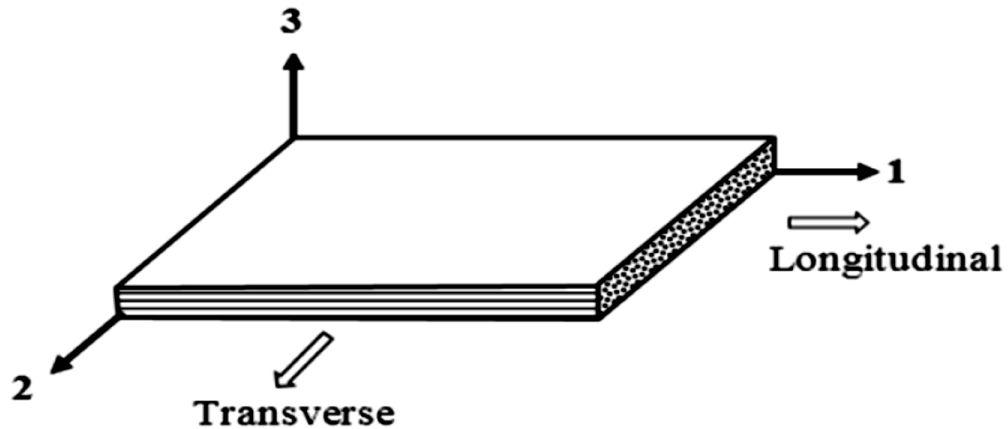


Figure 23 Schematic of unidirectional FRP lamina

The mechanical properties for the combined CFRP sheet and adhesive are evaluated using equations below as proposed by Mallick (1993).

$$E1 = E_f V_f + E_a (1 - V_f) \quad (3.10)$$

$$E2 = \frac{E_f E_a}{E_a V_f + E_f (1 - V_f)} \quad (3.11)$$

$$G12 = G13 = \frac{G_f G_a}{G_a V_f + G_f (1 - V_f)} \quad (3.12)$$

$$G23 = \frac{E2}{2(1 + \nu23)} \quad (3.13)$$

$$v_{23} = v_f V_f + v_a(1-V_f) \quad (3.14)$$

$$\sigma_{co} = V_f \sigma_u + ((1-V_f)E_a/E_f) \sigma_u \quad (3.15)$$

where:

E₁ : Elastic modulus in the longitudinal direction

E₂: Elastic modulus in the transverse direction

G₁₂ and G₁₃ : Plane shear modulus

G₂₃ : Normal to the plane shear modulus

v: Poisson's ratio

σ_{co} : Ultimate tensile strength

E_f : Elastic modulus of CFRP

V_f : Volume fraction of CFRP is provided by the manufacturer

E_a : Elastic modulus of adhesive material

G_f : Shear modulus of CFRP

G_a : Shear modulus of adhesive material

The properties of CFRP and epoxy used to strengthen the joints are listed in Tables 3 and 4, respectively. For the combined FRP sheets and the adhesive material, a summary of their mechanical properties is included in Table 5. It should be noted that the combined

thickness is calculated experimentally by the authors, and found to be twice the thickness of the fiber which is equal to 0.25mm.

Table 3 Properties of FRP sheets for joints BCJ-CFRP

Fiber type	Ultimate tensile strength (MPa)	Ultimate strain (%)	Modulus of elasticity (MPa)	Thickness (mm)
CFRP	3400	1.45	233300	0.125

Table 4 Properties of epoxy for installing FRP sheets for joints BCJ-CFRP

Epoxy type	Tensile modulus (MPa)
Epoxy for installing CFRP	3100

Table 5 Properties for combined CFRP sheets with matrix for joints BCJ-CFRP

Combined thickness (mm)	E1 (MPa)	E2 (MP)	v12	G12 (MPa)	G13 (MPa)	G23 (MPa)	σ_{co} (MPa)
0.25	96600	5190	0.3	1884	1884	1990	1550

3.3 Boundary Conditions

Different contact models could be used to model the interfacial region depending on the actual behavior and degree of accuracy. Tie contact is used between parts of beams and column. This type of contact is also used between loading plate and beam and this contact considers perfect bond between the two connected elements. At the same time, the contact between reinforcement and concrete is assumed perfectly bonded surfaces with no slip. This is justified by the enough development length of rebar and available friction between them, so embedded region contact is used to simulate the perfect bond. The column is assigned a pin support at its bottom end to restrain translation of the point in the three orthogonal directions (X, Y, Z). At the opposite end, a roller is assigned to prevent translation along only (X and Z) directions. Figure 24 also illustrates the Schematic view of boundary conditions and loads

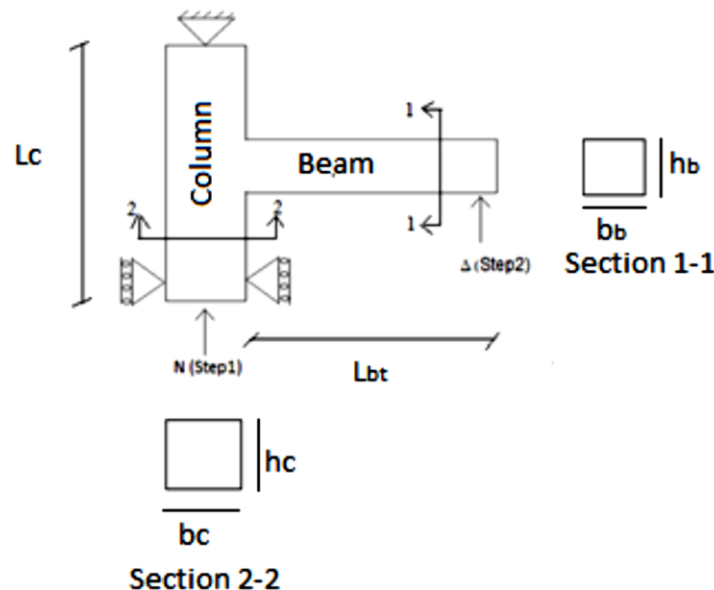


Figure 24 Schematic view of boundary conditions and loads

The static analysis method is used for the simulation of the loads. At the beginning, the top point of the column is subjected to a constant axial load of (2 MPa), similar to what was done in the experimental test. This is followed by applying a monotonically increasing displacement at the beam tip to investigate the resulting path of the load-deflection curve. In order to prevent local distortions, direct application of the boundary restraints as well as loads to the surface of concrete is avoided. They are instead applied to rigid plates inserted as intermediate parts.

3.4 Meshing

The components of beam-column joint are meshed individually on part-by-part basis instead of using global or sweep mesh. Eight-noded linear brick element (C3D8R) is used to model the solid elements; concrete and loading plate. A 2-node linear 3-D truss element is used to model main and transfers reinforcement (T3D2), whereas 4-noded shell element (S4R) used to model CFRP as shown in Figure 25.

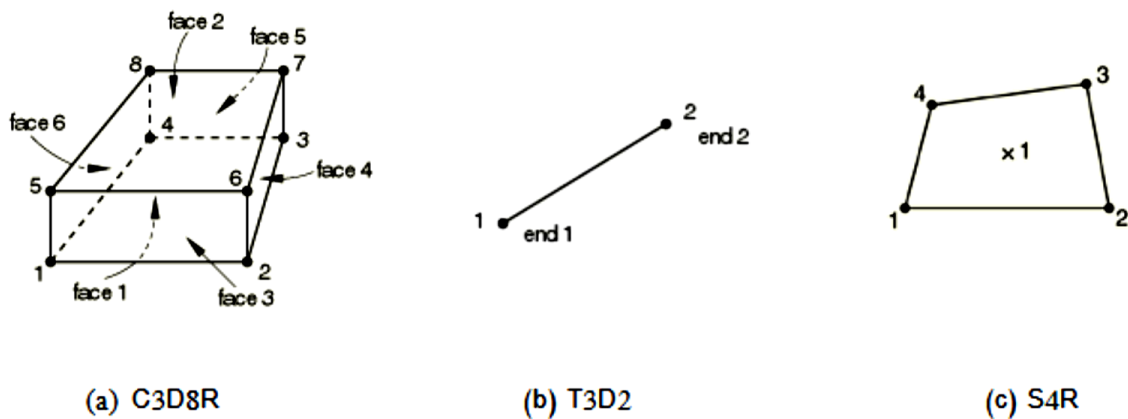


Figure 25 Elements used in the FE model

In order to eliminate the effect of mesh size on the results, a sensitivity study was conducted. Materials parameters are assumed same Jape et al. (2021) test different global mesh sizes were considered (15 mm through 45mm). The results show that the resulting curves stabilize approximately for meshes of range sizes 15-35 mm as shown in Figure 26 However a mesh size of 15 mm is used in all subsequent models to prevent excessive deformation error in ABAQUS which occurs in many models of 35/25 mesh sizes.

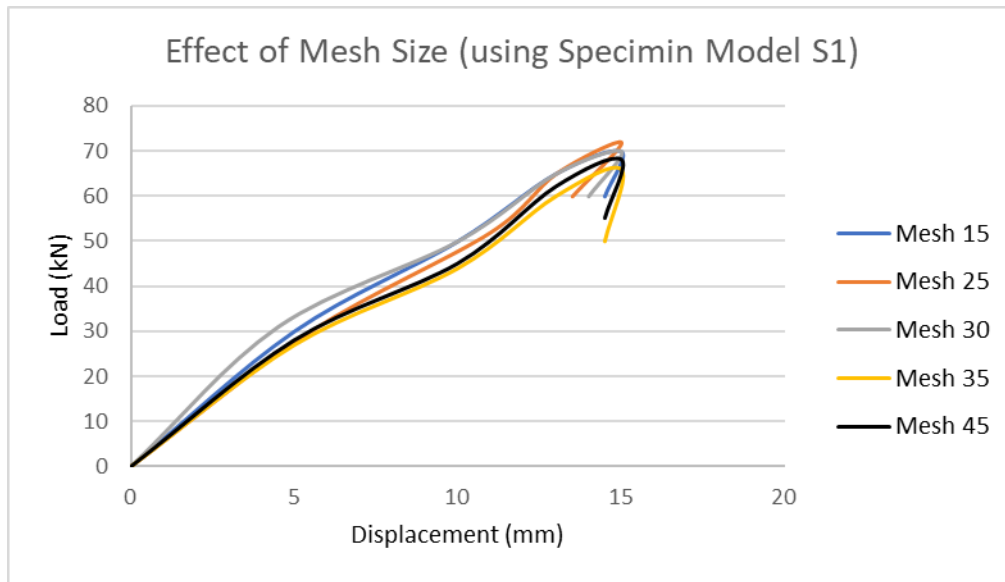


Figure 26 Mesh Size Effect

Chapter 4: Results and Analysis

4.1 Model Verification

To validate the results from the finite element model, data from experimental tests are used to conduct the verification. However, there are many experiments concerning R.C beam-column joints. Many of these experiments were not reported in details and this makes it difficult to model them. A set of clearly reported experiments are selected to validate the results of F.E models. Eight independent tests from literature review from (Jape et al, 2021) are used to conduct the verification. All of them are exterior R.C beam-column joint subjected to cycling loading which was tested experimentally, four specimens S1, S2, S3 and S4 are not strengthened with CFRP sheets, and RS1, RS2, RS3 and RS4 are retrofitted with FRP sheets, the following figure 27 presents the

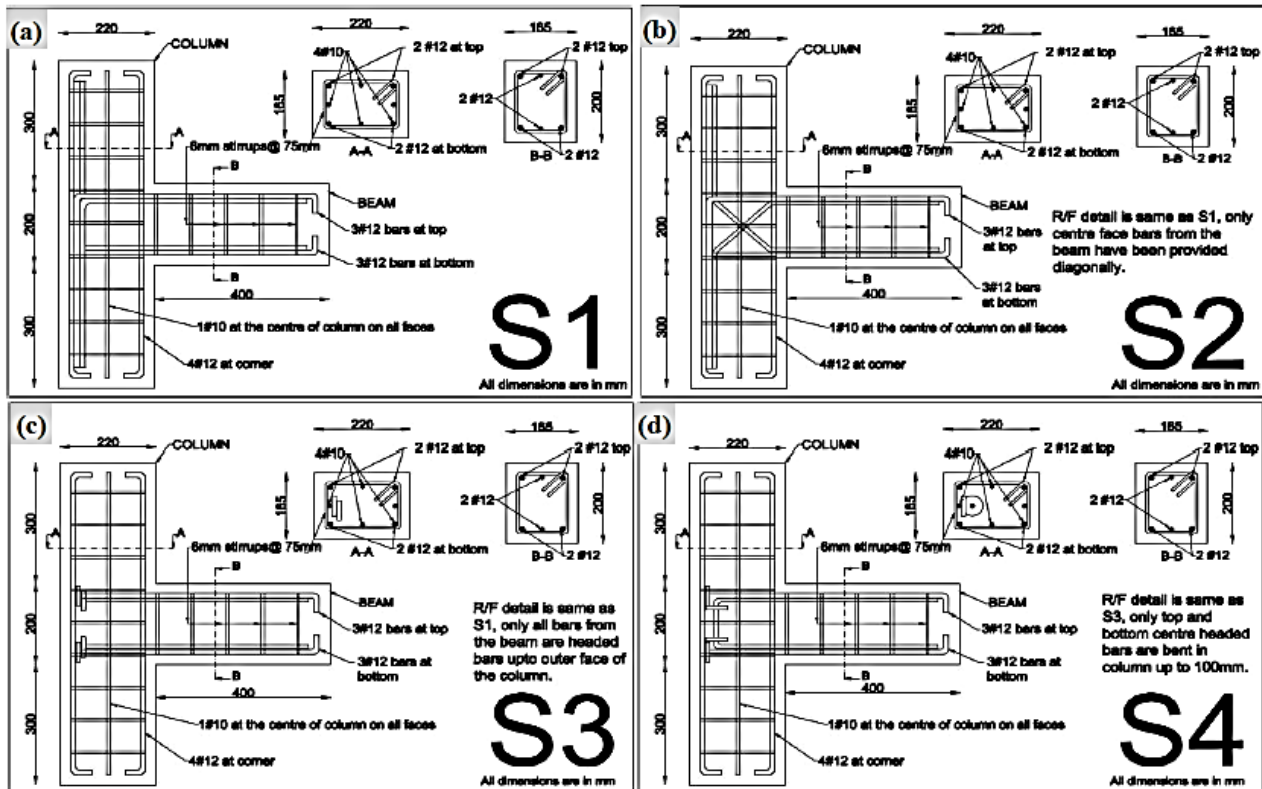


Figure 27 Reinforcement Details

The testing arrangement of the specimens are shown in the following figure 28:



Figure 28 Test Set up

4.2 Load displacement curves for control specimens

Figure 29 shows the load-displacement curve of the beam column joint specimen S1 tested by (Jape et al, 2021), the load-displacement curves are in good agreement, the model is verified and can be moved to next step the retrofitting with CFRP sheets.

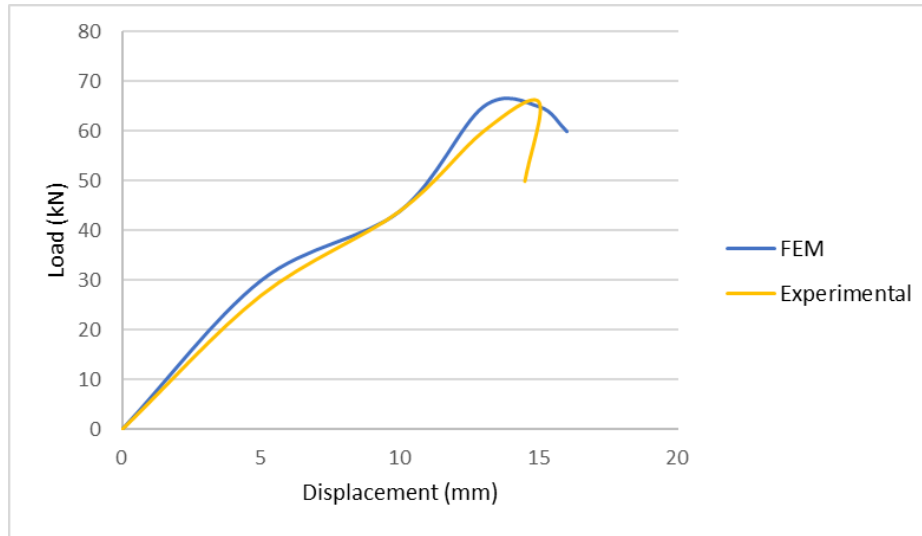


Figure 29 Verification of Control Specimen

4.3 Crack Patterns of specimens

The general cracking pattern for the non-retrofitted specimens S1, S2, S3 and S4 under reverse cyclic loading is as shown in Figure 30, from which it is observed that, flexural cracks appeared at the beam bottom face close to the beam column joint interface during the positive loading cycles. The same happened at the top surface of beam during the negative loading cycle. The cracks were almost symmetrical on both the faces of the beam column joint. At the lower stages of loading for the entire four specimens, minor shear cracks initiated diagonally at the joint interface and propagated in the joint region. Also, some inclined shear cracks were observed in the beam portion. However, cracks in the column were much less than those in the beam. This may be due to the column is subjected to a high axial compressive load; the net tensile stresses which may lead cracking in the column are quite small. Further, some vertical cracks were also observed in the beam, which may be occurred due to high flexural moments in the beam at higher stages of loading. All specimens behaved in the same manner with widening of diagonal shear cracks at the joint interface and cracks in the beam portion, ended at joint interface.

In case of S1 and S4 specimen, a greater number of finer cracks was developed in joint region, at the joint interface and in the beam portion. The joints were finally failed due to expansion of these cracks. However, in S1 specimen, crushing of concrete at the top of column was observed where the column was hinged. Now, in S2 specimen major crack widening was observed at the loading point which resulted in the failure of the S2 specimen. Similarly, S3 specimen also failed due to crack occurred at the loading point. This type of failure was different than failure of S1 and S4 specimen. Figure 30 shows the experimental crack pattern.



Figure 30 The experimental crack pattern.

Figure 31 presents the crack pattern of the joints modelled using ABAQUS, it presents the same crack pattern occurred for all non-strengthened RC beam column joint.

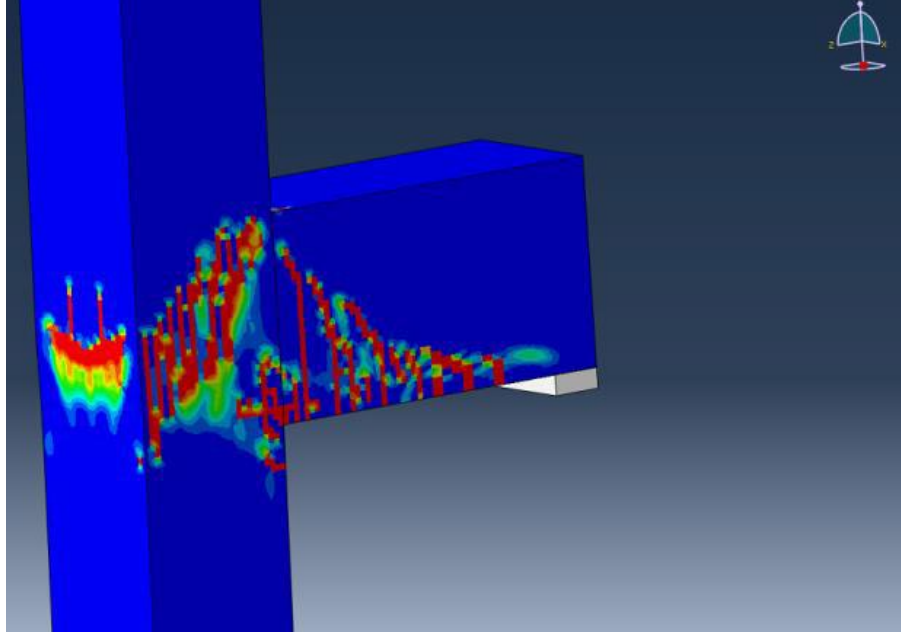


Figure 31 FEM crack Pattern

Experimentally, the case of any damaged members, the first step was to rebuild the damaged member. Damaged specimens S1, S2, S3, and S4 were first cleaned and made ready for retrofit. All cracks, voids, and irregular surfaces are finished with the help of putty. Putty is applied to smooth out the discontinuity, contaminants. When the putty was cured, a low viscosity primer coat of JSRprime is applied with the help of roller and brush, within the pot life period of 45 minutes of the mixture. JSRprime is a two-component adhesive system comprises a colorless base epoxy resin and amber-colored hardener as shown in Figure 32, both are mixed in a ratio of 100(Base):50(Hardener) by weight as per the manufactures instruction manual. Primer is applied to promote adhesive bonds for saturating resin. The inappropriate ratio would result in inferior end properties. The mixture is stirred to ensure full homogeneity. It is then allowed to cure.

When primer was fully cured, unidirectional JSRwrap (carbon fibre reinforced composite) was applied with JSRepoxyS Resin system. In a clean area away from resin carbon fibre reinforced composite is measured and cut as shown in Fig. 32. JSRepoxyS

Resin system is a moderate viscosity liquid Epoxy Resin. It is comprised of base resin (saturant) and hardener system mixed in ratio of 100(Base):2(Hardener) by weight as shown in Figure 32 The resin provides good pigment wetting and fibre cloth wetting with high level of mechanical and chemical resistance properties in the cured state.

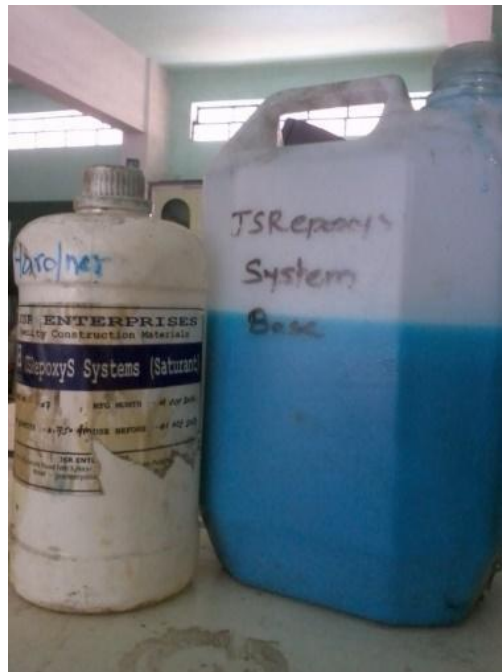
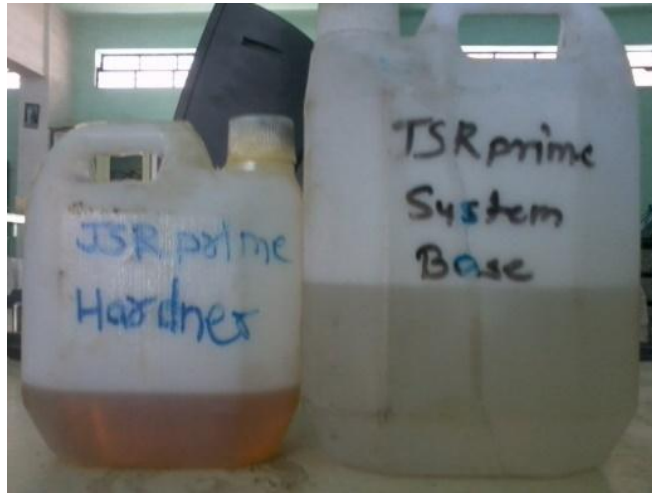


Figure 32 Resin and Hardener

4.4 Load displacement curves for strengthened specimens

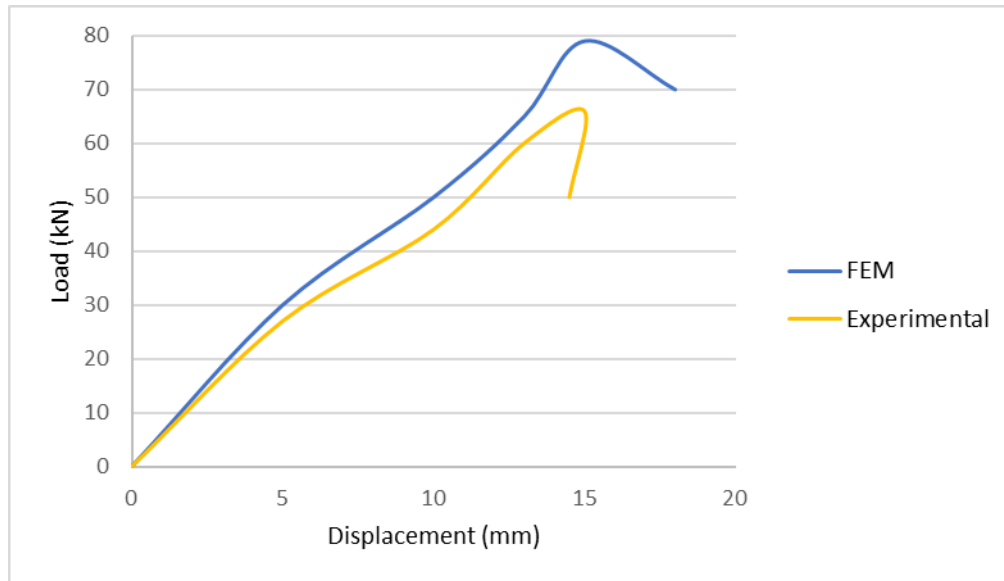


Figure 33 FEM Vs Experimental for repaired specimen RS1

The previous figure 33 shows the comparison between FEM results and experimental results for the retrofitted specimen RS1, It is clear that the FEM results gave greater maximum load than the experimental one, this was due to the brittle mode of failure occurred by the experimental test by the debonding of the CFRP sheets, in the model this was not a concern as it was not integrated in the model, this would give us a hint of the increase in the load capacity of the beam column joint that can be obtained if the mode of failure was assured to be ductile and not brittle.

4.5 Parametric study

4.5.1 Effect of CFRP with different f_c' values

Figures 34-36 presents the CFRP effect with different f_c' values for specimen 1 S1 which was not repaired with CFRP while RS1 which was repaired with CFRP, it is clear that the increase of CFRP compared to non-repaired specimen was at its maximum value when the $f_c'=32$ MPa (almost 33% increase percentage was found in load capacity of the BCJ due to the addition of CFRP sheets)

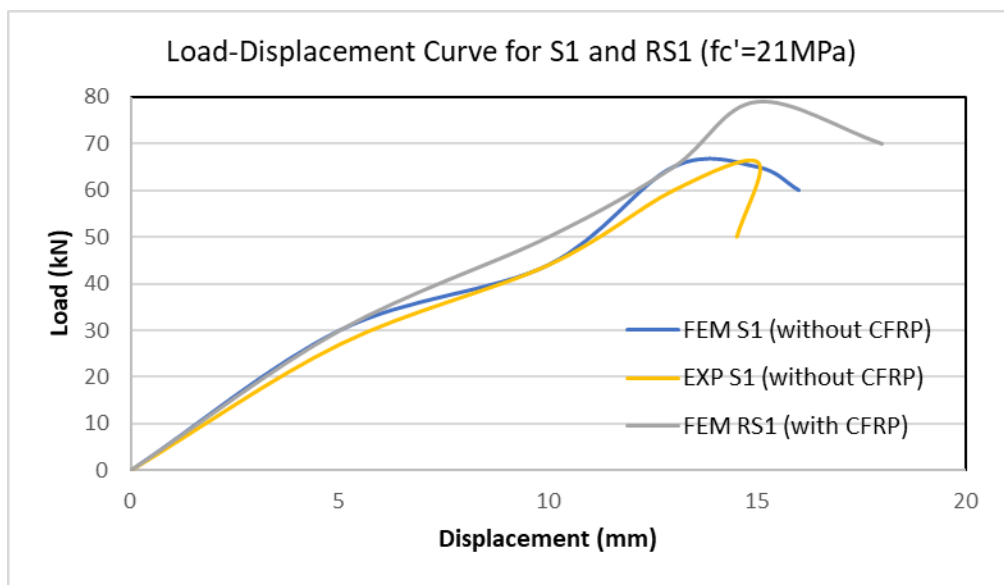


Figure 34 Load-Displacement Curve for repaired and non-repaired specimens ($f_c'=21$ MPa)

The increase percentage due to the addition of CFRP sheets was found to be 20 % when $f_c'=21$ MPa and 27 % when $f_c'=40$ MPa, it is clear that increasing the compressive strength over 40 MPa will not give higher percentage values due to the addition of CFRP sheets.

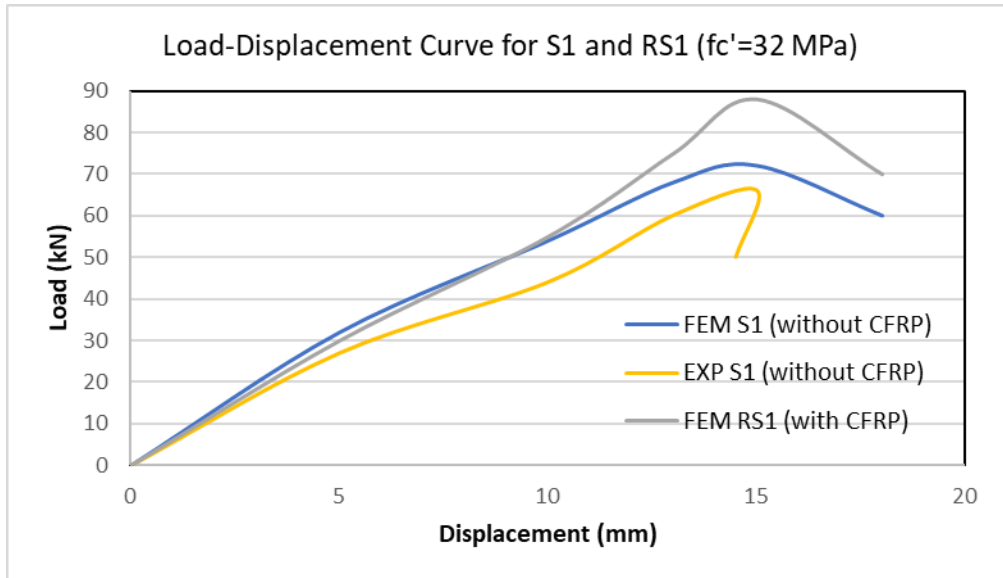


Figure 35 Load-Displacement for repaired and non-repaired specimens ($f_c' = 32$ MPa)

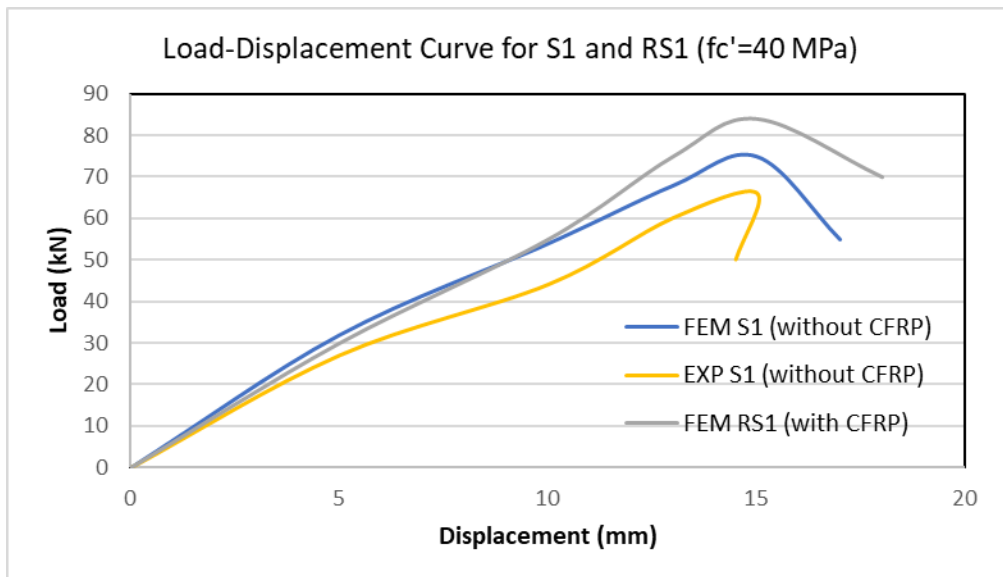


Figure 36 Load-Displacement for repaired and non-repaired specimens ($f_c' = 40$ MPa)

The following figures 37-39 show the Load-displacement curves for specimens S2 (non-strengthened) and RS2 (strengthened), it is clear that the CFRP sheets increased the ultimate displacement (ductility of the BCJ's) by almost 33 %. The FE model well captured the strengthened specimen behavior even the FEM gave greater load values than experimental, due to the early mode of failure happened experimentally which was discussed before. The increase due to CFRP sheets when $f_c'=21\text{MPa}$ was 17 %

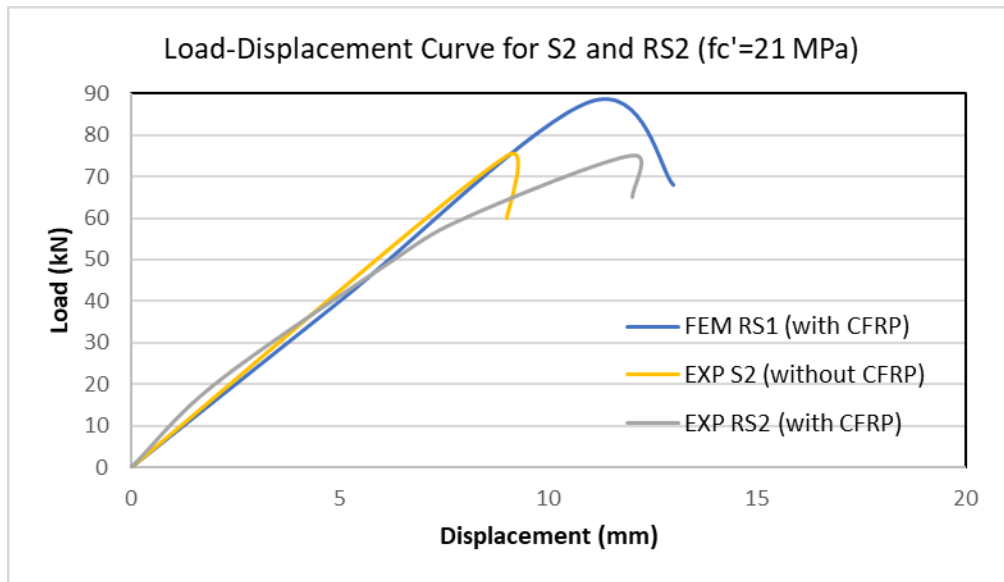


Figure 37 Load Displacement FEM VS experimental for RS2 ($f_c'=21\text{MPa}$)

The increase percentage due to CFRP sheets for S2 was found to be 30% for $f_c'=32\text{MPa}$ as shown in the following figure.

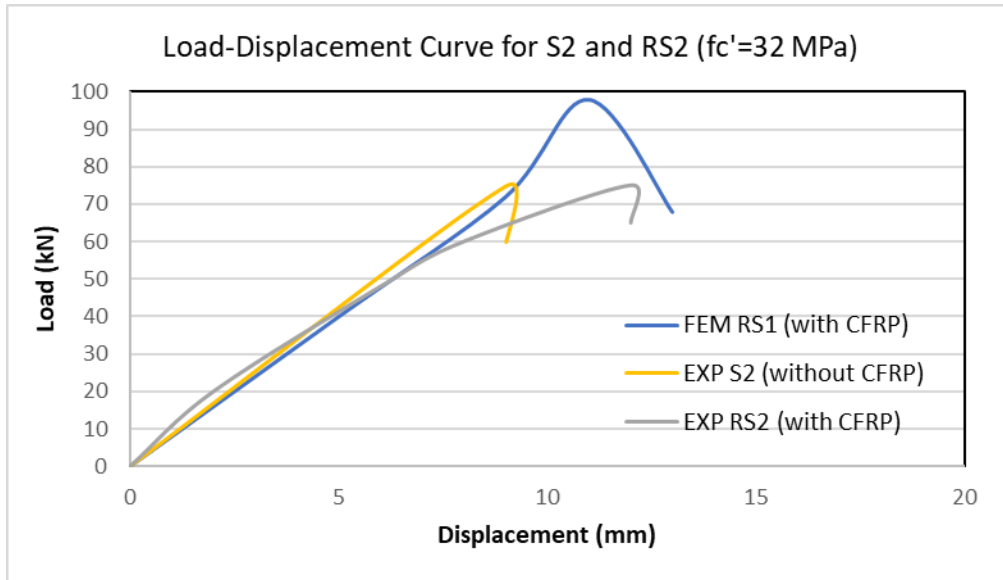


Figure 38 Load Displacement FEM VS experimental for RS2 ($f_c'=32$ MPa)

The increase percentage due to CFRP sheets for S2 was found to be 21% for $f_c'=40$ MPa as shown in the following figure 39.

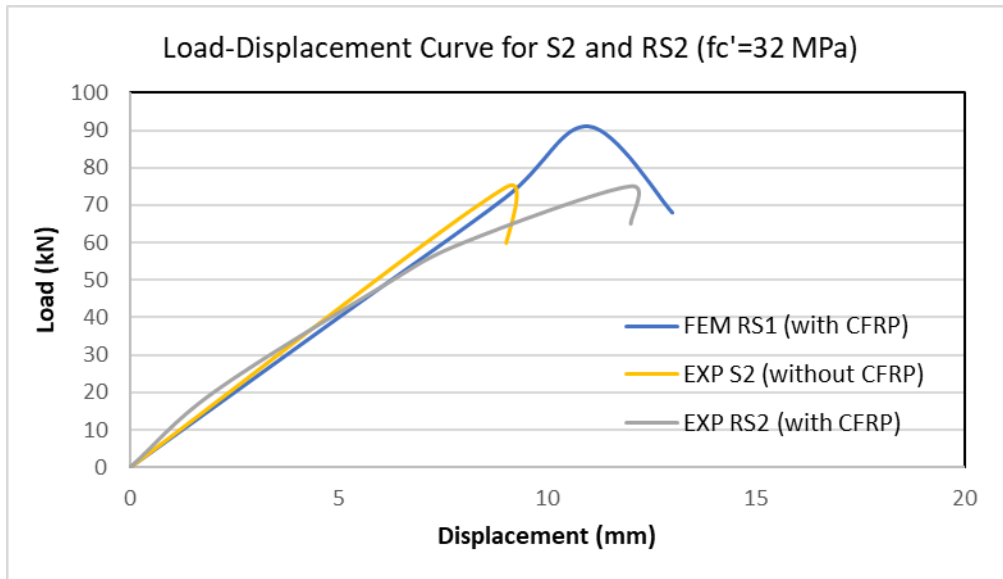


Figure 39 Figure 38 Load Displacement FEM VS experimental for RS2 ($f_c'=40$ MPa)

4.5.2 Stiffness of BCJ's

It is clear that the Stiffness of the specimens which were repaired with CFRP sheets was increased compared to non-repaired specimens, the following figure 40 shows the load - displacement at the first stage of loading (0-5 mm displacement) for specimens S2 and RS2

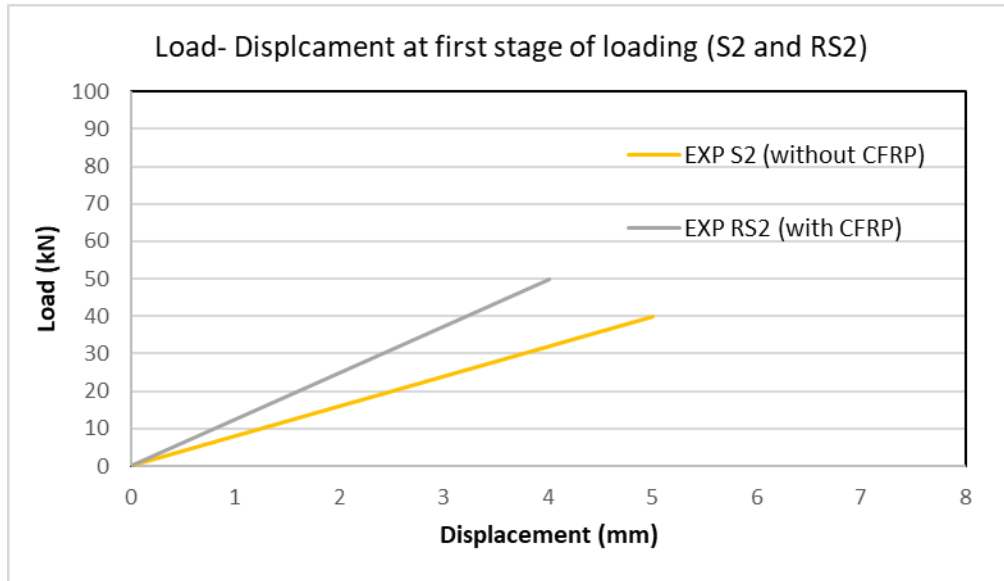


Figure 40 load -displacement at the first stage of loading

Figure 41 shows the values of the stiffness (the slope value before the yielding point is reached) for each BCJ before and after the repair process (stiffness ratio).

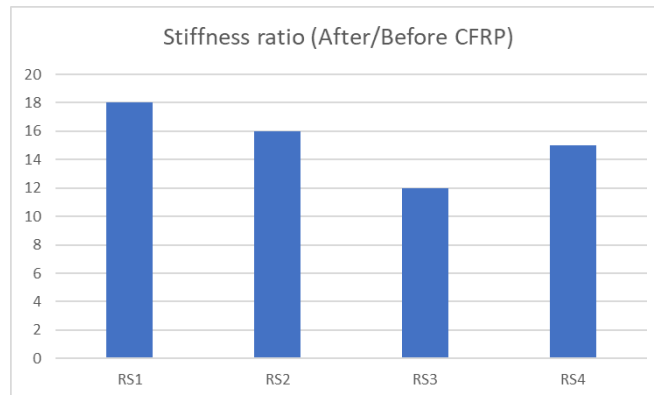


Figure 41 Stiffness Ratio

Chapter 5: Conclusions and Recommendations

Based on this thesis results which discussed several previous experimental results and conducted a FE model using the commercial software ABAQUS, the following remarks can be concluded:

- 1- Using CFRP sheets converts the brittle mode of failure to ductile failure. This result was found both in experimental review study and also by the FE model for the repaired BCJ's. However, the previous experimental results found that there was no important effect of CFRP sheets in terms of load capacity when failure in joints occurs inside the joint. On the other hand, the effect of CFRP sheets were found to be important when the failure mode was controlled by shear cracks.
- 2- The FEM model was verified using the control specimen, the repaired specimen did not give higher load capacity values in the experimental context due to the premature mode of failure occurred by the debonding of the CFRP sheets, the CFRP strengthening technique was not employed well in the experimental program, while on the other hand the FE model for the strengthened specimen gave higher load capacity value than the non-repaired specimen and that as the debonding of CFRP sheets was not a concern in this FE model.
- 3- The FE model results gave a satisfactory result in terms of load-displacement curves and failure/crack patterns, the FE model well captured the behavior of the BCJ's found by the experimental results and reached the almost the same ultimate load and displacement capacity values.
- 4- The increase percentage of CFRP effect compared to non-repaired specimen was at its maximum value when the $F_c' = 32$ MPa (almost 33% increase percentage was found in load capacity of the BCJ due to the addition of CFRP sheets), increasing

the compressive strength over 40 MPa did not give higher percentage values due to the addition of CFRP sheets.

- 5- The CFRP sheets increased the ultimate displacement (ductility of the BCJ's) by almost 33 % which was found by the FE model results, the stiffness was also restored for repaired specimens, the stiffness ratio values were between 12 and 18.

This master thesis focused on the exterior R.C beam-column joint without secondary beams, it is recommended to consider the effect of secondary beams and other types of joints like interior joints in any further studies.

Furthermore, it is recommended to consider the effect of adding contact element in order to consider the debonding mode of failure of the CFRP sheets to the concrete surface.

References

- ABAQUS: Abaqus analysis user's manual, Version 6.13 (2013). Assault Systems.
- ACI-ASCE (1985), —Recommendations for Design of Beam-Column Joints in Monolithic Reinforced Concrete Structures, Committee report 352R-85, American Concrete Institute, ACI Journal, Vol. 82, No 3, 266.
- Almassri, B. and Halahla, A.M., 2020, October. Corroded RC beam repaired in flexure using NSM CFRP rod and an external steel plate. In Structures (Vol. 27, pp. 343-351). Elsevier.
- Asran, G., EL-Esnawi, H. and fayed, S. (2016), —Numerical Investigation of RC Exterior Beam Colum Connections under Monotonic Loads, Journal of Mechanical and Civil Engineering.
- Beres, A., El-Borgi, S., White, R.N., Gergely, P., 1992. Experimental results of repaired and retrofitted beam-column joint tests in lightly reinforced concrete frame buildings, in: Experimental Results of Repaired and Retrofitted Beam-Column Joint Tests in Lightly Reinforced Concrete Frame Buildings. pp. 69–69.
- Bidgar, S. T. and Bhattacharya, P. (2014), —Nonlinear Finite Element Analysis of Reinforced Concrete Exterior Beam Column Joint Subjected to Monotonic Loading, RTCET STM J, 4(2), 1-10.
- Bracci, J.M., Reinhorn, A.M., Mander, J.B., 1995. Seismic retrofit of reinforced concrete buildings designed for gravity loads: performance of structural model. Structural Journal 92, 711–723.
- Campbell, F.C., 2010. Structural composite materials. ASM international.
- Cherry, S., Filiatrault, A., 1993. Seismic response control of buildings using friction dampers. Earthquake Spectra 9, 447–466.
- Corazao, M., Durrani, A.J., 1989. Repair and strengthening of beam-to-column connections subjected to earthquake loading. National Center for Earthquake Engineering Research.
- CSA A23.3 (1994), —Design of Concrete Structures, Canadian Standard Association, Rexdale, Ontario, Canada, 220 pages.
- Filiatrault, A., Lebrun, I., 1996. Seismic rehabilitation of reinforced concrete joints by epoxy pressure injection technique. Special Publication 160, 73–92.
- French, C.W., Thorp, G.A., Tsai, W.-J., 1990. Epoxy repair techniques for moderate earthquake damage. Structural Journal 87, 416–424.
- Ghobarah, A., Aziz, T.S., Biddah, A., 1996. Seismic rehabilitation of reinforced concrete beam-column connections. Earthquake Spectra 12, 761–780.
- Ghobarah A., T. El-Amoury, Seismic Rehabilitation of Deficient Exterior Concrete Frame Joints. J. Composite Constr., 9(5) (2005) 408-416. doi:10.1061/(ASCE)1090-0268(2005)9:5(408).
- Ghobarah, A., Said, A., 2001. Seismic rehabilitation of beam-column joints using FRP laminates. Journal of earthquake engineering 5, 113–129.
- JAPE, GAYAKE, S.B. and DHAKE, P.D., 2021. Structural behavior of beam column joint retrofitted using carbon fiber reinforced polymer. Journal of Materials and Engineering Structures «JMES», 8(1), pp.47-59.

- Jankowiak T, Lodygowski T. Identification of parameters of concrete damage plasticity constitutive model. *Foundations of civil and environmental engineering*. 2005 Jun;6(1):53-69.
- Jing, L., Pam, H.J., Francis, T., 2004. New details of HSC beam-column joints for regions of low to moderate seismicity. Presented at the 13th world conference on earthquake engineering, Vancouver, Canada.
- Kaliluthin, A., Kothandaraman, S., Ahamed, T.S., 2014. A review on behavior of reinforced concrete beam-column joint. *International Journal of Innovative Research in Science, Engineering and Technology* 3, 11299–11312.
- Karayannis, C., Chalioris, C., Sideris, K., 1998. Effectiveness of RC beam-column connection repair using epoxy resin injections. *Journal of Earthquake Engineering* 2, 217–240.
- Kupfer, H., Hilsdorf, H.K. and Rüsç, H. (1969), —Behavior of Concrete Under Biaxial Stresses, *ACI Journal of structural Divisions*, Vol. 66, No. 8, pp. 656–666.
- KR, S.C., GS, T., 2012. Comparative Study on Behaviour of Reinforced Beam-Column Joints with Reference to Anchorage Detailing.
- Lee J, Fenves GL. Plastic-damage model for cyclic loading of concrete structures. *Journal of engineering mechanics*. 1998 Aug;124(8):892-900.
- Lubliner J, Oliver J, Oller S, Oñate E. A plastic-damage model for concrete. *International Journal of solids and structures*. 1989 Jan 1;25(3):299-326.
- Mallick, P.K. (1993), —Fiber-Reinforced Composites, Marcel Dekker, New York.
- Margalit, T., Mualam, N., 2020. Selective rescaling, inequality and popular growth coalitions: The case of the Israeli national plan for earthquake preparedness. *Land Use Policy* 99, 105123.
- Nayal R and Rasheed HA. Tension stiffening model for concrete beams reinforced with steel and FRP bars. *Journal of Materials in Civil Engineering* 2006;18(6):831-841.
- Naeim, F., Kelly, J.M., 1999. Design of seismic isolated structures: from theory to practice. John Wiley & Sons.
- Priestley, M., 1997. Displacement-based seismic assessment of reinforced concrete buildings. *Journal of earthquake engineering* 1, 157–192.
- A. Prota, A. Nanni, G. Manfredi, E. Cosenza, Seismic upgrade of beam-column joints with FRP reinforcement. *L'Industria Italiana del Cemento*, 70(11) (2000) 868-877.
- Pushkar, S., Halperin, I., Ribakov, Y., 2022. Combining an Intensive Green Roof with Seismic Retrofitting of Typical Reinforced Concrete Buildings in Israel. *Materials* 15, 889.
- Ribakov, Y., Halperin, I., Pushkar, S., 2018. Seismic resistance and sustainable performance of retrofitted buildings by adding stiff diaphragms or seismic isolation. *Journal of Architectural Engineering* 24, 04017028.
- Saenz LP. Equation for the Stress-Strain Curve of Concrete. *ACI Journal* 1964; 61(9): 1229–1235.
- Sharif, A.M., Samaaneh, M.A., Azad, A.K., Baluch, M.H., 2016. Use of CFRP to maintain composite action for continuous steel–concrete composite girders. *Journal of Composites for Construction* 20, 04015088.
- Wahalathantri, B. L., Thambiratnam, D. P., Chan, T. H. T. and Fawzia, S. (2011), —Material Model for Flexural Crack Simulation in Reinforced Concrete

- Elements Using ABAQUS[®], In Proceedings of the First International Conference on Engineering, Designing and Developing the Built Environment for Sustainable Wellbeing , pp. 260-264.
- Tsonos, Effectiveness of CFRP-jackets and RC-jackets in post-earthquake and pre-earthquake retrofitting of beam–column subassemblages. *Eng. Struct.*, 30(3) (2008) 777-793. doi:10.1016/j.engstruct.2007.05.008.
- United Nations Industrial Development Organization, 1983. *Repair and Strengthening of Reinforced Concrete, Stone and Brick Masonry Buildings*.
- Voyiadjis GZ and Taqieddin ZN. Elastic plastic and damage model for concrete materials: Part I – Theoretical formulation. *Int J Struct Changes Solids – MechAppl* 2009;1(1):31–59.